AN ABSTRACT OF THE DISSERTATION OF

Burke Thomas Greer for the degree of Doctor of Philosophy in Forest Ecosystems and Society presented on February 3, 2017.

Title: Differences in Evolutionary History and Ploidy Type Shape the Interactions of *Populus tremuloides* Michx. with Climate

Abstract approved:

_____

Christopher J. Still

Quaking aspen (*Populus tremuloides* Michx) is a species with high phenotypic plasticity and a broad distribution that, in the last decade, has experienced climate stress-induced mortality called Sudden Aspen Decline (SAD). In order to help mitigate the effects of SAD in the future, we need a better understanding of aspen's climate adaptation. We also need to learn more about how aspen structure and function relate to climate. To that end, this dissertation seeks to improve our understanding of aspen biogeography by exploring multi-scale genetic-climate interactions. First, we examined aspen climate adaptation, asking if genetic relatedness corresponded to any similarities or differences in climate niche across aspen's range. We found that two aspen sub-populations, with genetic differences, had distinctly different climate niches and we concluded that aspen species distribution models should include genetic relatedness to predict species range more accurately. We also studied how polyploidy in aspen affected the structure and function of leaves, branches, and ramets. We found that diploid and triploid aspen had differences in leaf traits that ultimately drove greater triploid maximum photosynthetic rates, stomatal conductance, and intrinsic water-use efficiency (*iWUE*). However, despite

greater *iWUE* in triploids, we found that they were actually more prone to climate-induced stress because of higher stomatal conductance rates and less stomatal sensitivity and control than diploids. Finally, we measured growth and *iWUE* in tree rings from diploid and triploid aspen. We learned that diploid growth had statistically significant positive correlations with total precipitation and the last day with snow on the ground. We also found that triploid growth had a statistically significant positive correlation with total precipitation, and a negative correlation with vapor pressure deficit. In addition, we found that while *iWUE* in both diploids and triploids increased during years with less available water, *iWUE* was nearly 4% greater in triploid aspen in every year. To maintain this ~4% greater *iWUE* when there was less available water, it is likely that triploid aspen did not reduce photosynthetic rates and stomatal conductance as much as diploids. Again, this suggests that triploids may be more prone than diploids to climate-induced stress because triploids require more water than diploids when there is less water available. Overall, our findings improve our understanding of macroscale and local scale interactions between aspen and climate.

Differences in Evolutionary History and Ploidy Type Shape the Interactions of *Populus tremuloides* Michx. with Climate

by
Burke Thomas Greer

A DISSERTATION

submitted to

Oregon State University

in partial fulfillment of
the requirements for the
degree of

Doctor of Philosophy

Presented February 3, 2017
Commencement June 2017

Doctor of Philosophy dissertation of Burke Thomas Greer presented on February 3, 2017

APPROVED:

Major Professor, representing Forest Ecosystems and Society

Head of the Department of Forest Ecosystems and Society

Dean of the Graduate School

I understand that my dissertation will become part of the permanent collection of Oregon State University libraries. My signature below authorizes release of my dissertation to any reader upon request.

Burke Thomas Greer, Author

ACKNOWLEDGEMENTS

First, I want to thank Chris Still for accepting me as a student and for bringing me here to Corvallis for my PhD. I also want to thank my committee members Steve Strauss, Renee Brooks, Rick Meinzer, and Ryan Contreras for your guidance, collaboration, and support. I also thank my wife, Renee Greer, for your endless help and support while I completed my PhD. I also thank my parents, Gordon and Meg Greer, my sister Marissa, and my extended family for their support while I kicked around academia for seven years. I also thank fellow RMBLers, graduate students, and friends from Santa Barbara to Corvallis to Boston for sharing hikes, trips into the mountains, or for simply sitting around a fire with me talking science and drinking a beer, or tying flies. Finally, I also thank fellow members of the TU Bluebacks Chapter in Corvallis and fellow anglers for working with me on local conservation projects, and for simply fishing with me.

Below are project-specific acknowledgements specific to each manuscript:

Populations of aspen (Populus tremuloides Michx.) with different evolutionary histories differ in their climate occupancy: Chris Funk at the University of California, Santa Barbara, contributed to the development of the project design and early manuscript preparation. Jerry Rehfeldt and James Worrall provided aspen presence and absence data that were critical to this study. The biomod2 forums managed by Damien Georges and Wilfried Thuiller provided troubleshooting and edits to the source code which aided the creation of the ensemble models. Terralyn Vandetta's technical expertise and support with the Rocks high performance computer cluster was also critical during the creation of the species distribution models. The Rocky Mountain Biological Laboratory, the

University of California, Santa Barbara, and Oregon State University have provided funding, workspace, and computing resources. Conversations with faculty, fellow students, and colleagues in Gothic, Corvallis, Santa Barbara and San Francisco have all shaped this manuscript. We also acknowledge comments from reviewers that greatly improved the manuscript.

Polyploidy in Quaking aspen (Populus tremuloides Michx.) influences plant-climate interaction and increases susceptibility to climate-induced drought stress:

We thank Steven Strauss who provided useful insight that guided study methods and interpretations of our data. We are thankful for the support of the Rocky Mountain Biological Laboratory in Gothic, Colorado, who provided funding and logistical support to B. Greer. B. Greer also would like to thank the science director, Jennifer Reithel, and the executive director Ian Billick for their support while scoping this project, collecting data, and summarizing our findings. We also thank the department of Forest Ecosystems and Society, in the College of Forestry, at Oregon State University for funding support. We also thank Jennifer McKay for completing our isotope analysis and we thank Lisa Ganio, and Ariel Muldoon for guidance in our statistical approaches. We thank Steven Voelker who provided useful comments that greatly improved the manuscript. Richard Cronn and Chris Poklemba also provided guidance while troubleshooting ploidy testing using flow cytometry and Patrick Hays provided barley leaves. This manuscript has been subjected to Agency review and has been approved for publication. The views expressed in this paper are those of the author(s) and do not necessarily reflect the views or policies of the U.S. Environmental Protection Agency. Mention of trade names or commercial products does not constitute endorsement or recommendation for use.

Triploid aspen have greater basal area growth and intrinsic water-use efficiency than diploid aspen, but are also at greater risk to drought and higher atmospheric water demand: We thank Steven Strauss for collaboration that helped improve the methods. We also thank Jennifer McKay for completing our isotope analysis. We are thankful for the support of the Rocky Mountain Biological Laboratory in Gothic, Colorado, who provided funding and logistical support to B. Greer. We also thank the department of Forest Ecosystems and Society, in the College of Forestry, at Oregon State University for funding support.

CONTRIBUTION OF AUTHORS

Populations of aspen (Populus tremuloides Michx.) with different evolutionary histories differ in their climate occupancy.

Greer, Burke Thomas; Still, Christopher; Howe, Glenn T.; Tague, Christina; Roberts, Dar A.

B.T.G., C.S., G.T.H, C.T., and D.A.R. conceived the research. B.T.G. and C.S. designed the research. B.T.G. performed the research, data collection, and data analysis. B.T.G., C.S., G.T.H, C.T., and D.A.R. all contributed to writing the manuscript.

Polyploidy in Quaking aspen (Populus tremuloides Michx.) influences plant-climate interaction and increases susceptibility to climate-induced drought stress.

Greer, Burke T.; Still, Christopher; Cullinan, Grace L.; Brooks, J. Renée; Meinzer, Frederick C.

B.T.G, C.S., G.L.C., R.J.B, F.C.M. designed the research. B.T.G. and G.L.C. performed the research and data collection. B.T.G. completed the data analysis. B.T.G, C.S., G.L.C., R.J.B, F.C.M. all contributed to writing the manuscript.

Triploid aspen have greater basal area growth and intrinsic water-use efficiency than diploid aspen, but are also at greater risk to drought and higher atmospheric water demand

Greer, Burke T.; Still, Christopher; Voelker, Steve; Brooks, J. Renée; Meinzer, Frederick C.

B.T.G., C.S., S.V, J.R.B and F.C.M designed the research. B.T.G. performed the research, data collection, and data analysis. B.T.G, C.S., S.V., R.J.B, F.C.M. all contributed to writing the manuscript.

TABLE OF CONTENTS

TABLE OF CONTENTS (CONTINUED)

TABLE OF CONTENTS (CONTINUED)

LIST OF FIGURES

LIST OF TABLES

LIST OF APPENDICES

LIST OF APPENDIX FIGURES

Figure Page

LIST OF APPENDIX TABLES

1. Introduction

Quaking aspen have a native range that extends across huge swaths of North America, including regions of central Alaska, Newfoundland, Utah, Colorado, California, Michigan, Mexico, and a myriad of places in between (Burns & Barbara, 1990). This broad biogeography is usually attributed to aspen's life history strategies, and high genetic diversity and phenotypic plasticity (Mitton & Grant, 1996). Quaking aspen are wind pollinated and dispersed, and seeds can travel tens of kilometers with the breeze (Mitton & Grant, 1996; Romme et al., 1997; Turner et al., 2003). Aspen are also dioecious and different genders of aspen may be adapted to different landscape positions which diversify aspen's niche (Grant & Mitton, 1979). After an aspen seed has established, an aspen grows its first stem (ramet), and grows lateral roots that are within 20 to 45 centimeters of the soil surface. After the first growing season, these lateral roots can grow new stems, and further spread into the surrounding area. This process is called 'cloning by root sucker', and over time can result in extensive aspen clones with shared genetic heritage that are single organisms (B. V. Barnes, 1975; B.V. Barnes & Wagner, 2002; Grant & Mitton, 1979; Kemperman & Barnes, 1976; Mitton & Grant, 1996; Mock et al., 2008). In fact, Pando, the largest aspen clone in the world, and possibly the world's largest organism (measured by biomass), is estimated to have more than 47,000 ramets, and has grown to greater than 43 ha in area (Kemperman & Barnes, 1976; Mock et al., 2012). Quaking aspen is also a primary successional species that can disperse to and colonize distant sites after disturbances like forest fires. For example, aspen replaced Lodgepole pine after the 1988 Yellowstone Fire with the nearest mature aspen stand to

the burn scar being nearly 5 km away (Romme et al., 1997; Turner et al., 2003)). Over longer periods, aspen can be replaced by more shade-tolerant species (like Douglas-fir or Lodgepole pine), but may also live in stable aspen-dominated stands (Burns & Barbara, 1990; Mitton & Grant, 1996). There is still much to be learned about aspen, but its ability to disperse in the landscape, and to clone and regrow from roots once they've established, contribute to its broad distribution

Climate tolerance (often quantified as climate niche) is a constraint to the distribution of species and is a function the phenotypes of each individual of that species and their respective environments (Bonan, 2002; Franklin, 2010, 2013; Levitt, 1980). Phenotype (and thus plant structure and function) is determined by the genetics of a plant as it interacts with its biotic and abiotic environment over time and space (Bonan, 2002; Lande & Shannon, 1996; Levitt, 1980). In aspen (and other clonal plants), these determinants of phenotype are complicated by the fact that aspen ramets in the same clone are genetically similar while microscale climatic environments for each ramet in that clone may vary or stay the same depending on the landscape, clone size, and time (B. V. Barnes, 1975; Kemperman & Barnes, 1976; Mock et al., 2008). Furthermore, quaking aspen are often polyploid which introduces an additional dynamic to the distribution of this species because polyploidy can change gene expression, and thus phenotype (Barker et al., 2016; Madlung & Wendel, 2013; Maherali et al., 2009; Mock et al., 2012; Segraves & Anneberg, 2016; Soltis et al., 2014). In fact, in aspen, it has been found that northern populations are virtually 100% diploid and southern populations are up to 69% triploid (Mock et al., 2012). One theory for this biogeographical pattern is that polyploids may be

better suited than diploids to dry and warm climatic conditions (Mock et al., 2012). These ploidy-related biogeographical patterns in aspen follow other species where ploidy types sort along climate gradients. For example, wild potato (*Solanum* section *Petota*) triploids have been found to live in warmer and drier climates than diploids, while tetra-, penta- and hexaploids are found in cooler, and wetter places (Hijmans et al., 2007). Also, creosote (*Larrea tridentata*) diploid, tetraploid, and hexaploid ploidy levels align to gradients of summer temperature and precipitation with hexaploids being the most tolerant of hot, dry summers, while diploids are the least tolerant and tetraploids are intermediate (Hunter et al., 2001). In other species, polyploidy modifies traits that increase drought and heat stress tolerance or avoidance that might increase relative fitness while differentiating niche between ploidy types. For example, ploidy types of *Atriplex canescens* vary relative to soil water availability with hexaploids being most frequent in fine textured soils with low water permeability and from which water is more difficult to extract (Dunford, 1984). This is likely because higher ploidy levels confer greater resistance to drought-induced loss of stem hydraulic conductivity and therefore have greater drought resistance (Hao et al., 2013). Another way that plants can tolerate drought impacts is by expressing increased intrinsic water-use efficiency (*iWUE*). *iWUE* is the ratio of carbon assimilation, *A*, to stomatal conductance, g_s and can be modeled using carbon isotope discrimination, $\delta^{13}C$, to calculate *iWUE* (G.D. Farquhar et al., 1982; G. v. Farquhar et al., 1980; Seibt et al., 2008). By either increasing *A* relative to changes in g_s, or decreasing g_s relative to changes in *A*, *iWUE* can be increased. This can be achieved through changes to plant structure. For example, increasing chlorophyll content per leaf

area might increase *A*, or reducing stomatal size might reduce g_s, (Bonan, 2002). In theory, a plant with greater *iWUE* could tolerate drought better because they maximize the efficiency of their carbon gain to water loss (Nicotra & Davidson, 2010). This is likely in the case of the annual grass, *Brachypodium distachyon*, whose polyploids have both greater *iWUE,* and increased drought tolerance compared to diploids (Manzaneda et al., 2012).

Despite aspens' general phenotypic plasticity, widespread climate-driven mortality, deemed Sudden Aspen Decline (SAD), is a threat to aspen forests in North America. The most recent and most famous bought of SAD occurred in the Southwestern United States following warm and dry weather in 2002 and 2003, affecting trees in Colorado, Utah, Arizona and New Mexico (Worrall et al., 2008; Worrall et al., 2010; Worrall et al., 2013). SAD is characterized by whole-ramet and root mortality from hydraulic failure and at landscape scales was most prevalent where ground-water supply was lowest in areas like slope-shoulders (L. D. Anderegg et al., 2013; Anderegg et al., 2014; Anderegg et al., 2012; W. R. Anderegg et al., 2013; Worrall et al., 2013). Resampling in two long-term forest plots in Colorado found that, post-SAD, there were 25% fewer aspen and aspen stand density and basal area were 32% lower (Bretfeld et al., 2016; Coop et al., 2014). As climate change continues, future SAD events are expected and this could have wide-reaching impacts on North American forests because aspen are so widespread (Rehfeldt et al., 2009; Worrall et al., 2013).

In order to understand and help mitigate the effects of SAD on the forests of North America, it is clear that we need a better understanding of the mechanisms that drive

aspen biogeography. In this work, I explored two main themes regarding aspen-climate interaction. First, I asked if genetically similar sub-populations of quaking aspen were adapted to the same or different climates by comparing aspen's climate niche between two subpopulations. Through this approach, I was able to measure if genetic relatedness corresponded to similarities or differences in climate niche or climate adaptation. Second, I asked if there were differences in diploid and triploid aspen structure and function that explained potential differences in ploidy-climate interactions. I found structural and functional differences between ploidy types that show that while triploid aspen have greater net carbon uptake and *iWUE*, they are actually more prone than diploid aspen to climate-induced stress because of higher potential transpiration rates. Ultimately, through our research, we gained a greater understanding of mechanisms that drive aspen's biogeography.

Populations of aspen (*Populus tremuloides* Michx.) with different evolutionary histories differ in their climate occupancy

Greer, Burke Thomas; Still, Christopher; Howe, Glenn T.; Tague, Christina; Roberts, Dar A.

Ecology and Evolution
Volume 6, Issue 9: 3032-3039

2. Populations of aspen (*Populus tremuloides* Michx.) with different evolutionary histories differ in their climate occupancy

2.1 Abstract

Quaking aspens (*Populus tremuloides* Michx.) are found in diverse habitats throughout North America. While the biogeography of aspens' distribution has been documented, the drivers of the phenotypic diversity of aspen are still being explored. In our study, we used species distribution models to characterize the climate niche of the entire population of quaking aspen, and two sub-populations of aspen, and measured niche overlap between each population. We found that northern and southwestern populations occupy different climate niches, and our results support the inclusion of genetic and phenotypic data with species distribution modeling for predicting aspens' distribution.

2.2 Introduction

Quaking aspen (*Populus tremuloides* Michx.) thrives in a variety of landscapes across North America. In the Intermountain West and Rocky Mountains, aspens are found in dense groves with spruce and fir at middle elevations, and in pure stands or in isolated groves at tree line (W. Shepperd et al., 2000). At its lowest elevations in Nevada and Utah (150 to 300m), aspens are found in riparian corridors (Mueggler, 1988). In the Sierra Nevada Mountains of California, aspens are found in riparian corridors, on slopes, and in isolated pockets and krümmholz stands (W. D. Shepperd et al., 2006). In contrast, North America's eastern and northern aspens are found most often at swamp and stream margins (B.V. Barnes & Wagner, 2002). In the southwest region of North America, aspens occur on sites typically fed by snowmelt, whereas in the north and east, they rely

on winter snowpack and summer rains (B.V. Barnes & Wagner, 2002). Unlike aspens in the southwest, northern aspens are only able to colonize upland sites when canopy openings become available following fire or other disturbances, and on these sites they are later outcompeted by other species (B.V. Barnes & Wagner, 2002).

Aspen stands are made up of one or multiple clones, which propagate through sexual reproduction using windblown pollen and seeds, and asexual reproduction through clonal growth from root suckering (B. V. Barnes, 1975; B.V. Barnes & Wagner, 2002; Mock et al., 2008). Although the Rocky Mountains are famous for their large clonal stands of aspen, large clonal stands are absent from the Great Lakes region and central Canada (Mitton & Grant, 1996). These differences suggest that asexual reproduction is much more common in the southwestern portion of aspens' range (Kemperman & Barnes, 1976), and that sexual reproduction occurs during short 'windows of opportunity' (Jelinski & Cheliak, 1992). Nonetheless, throughout its range, the sizes and distributions of aspen clones depend on the combined success of sexual and asexual reproduction (Mock et al., 2008).

Species distributions are constrained by evolutionary history, the ability and opportunity to disperse into new environments, the amount of adaptive phenotypic variation (including adaptation to climate), and gene flow among extant populations (Kirkpatrick & Barton, 1997). Analyses of neutral genetic markers suggest that aspens' current distribution has been weakly constrained by evolutionary history, while gene flow has been extensive. For example, analysis of range-wide genetic diversity using SSR markers

suggests that diploid aspens are weakly differentiated within the northern and southwestern portions of the species' range (Callahan et al. (2013). These "northern" and "southwestern" clusters are roughly separated by a boundary consisting of the maximum extent of the Pleistocene glaciation and the continental divide (see Figure 1 in Callahan et al 2013). Although the northern cluster was found to have greater genetic diversity, it had no strong geographical structure. This suggests that gene flow is high and/or the northern cluster resulted from a cohesive northward migration of populations during the retreat of the glaciers. The southwestern cluster is very different, having lower genetic diversity and greater geographical structure. The authors hypothesized that the southwestern cluster consists of "stable edge" populations—instead of moving northward, these populations seem to have migrated up and down the mountains and hillslopes tracking changes in climate. Additionally, Callahan et al. (2013) speculated that the northern and southwestern clusters are adapted to different climates because the northern cluster inhabits a mesic, continental climate, whereas the southwestern cluster inhabits a climate that is semi-arid.

Empirical information on aspens' adaptation to climate comes from analyses of climate envelopes and common garden studies. Range-wide climate envelopes have been characterized by Rehfeldt et al. (2009) and Worrall et al. (2013). Rehfeldt et al. (2009) found that aspens' distribution was primarily driven by three climate variables: an annual dryness index, the ratio of summer to annual precipitation, and an index incorporating growing season precipitation and growing degree days. Using an updated version of this

model, Worrall et al. (2013) found that maximum summer temperatures and summer precipitation (April-September) were the best predictors of aspens' range-wide distribution.

Traits associated with local climatic adaptation of aspen populations have been identified using common garden studies. For example, in a reciprocal transplant study in Alberta, Canada, tree diameter and height were strongly related to the latitudes from which each population originated (Gylander et al., 2012). In another reciprocal transplant study of ten aspen populations from western Canada and Minnesota, tree height, total biomass, and the timing of budbreak were strongly related to latitude (Schreiber et al., 2013), and in a related study, the timing of budbreak was associated with total growing degree days (H. T. Li et al., 2010). Finally, using a reciprocal transplant study and species distribution models, relationships between tree heights and climate variables were used to project the future growth of aspens for 2020, 2050, and 2080 under four Intergovernmental Panel on Climate Change (IPCC) emissions and population growth scenarios (Gray et al., 2011). However, because the study of Gray et al. (2011) was restricted to western Canada, it did not address larger scale differences between the northern and southwestern portions of aspen's range.

Given these aspen-climate relationships, and the work of Callahan et al. (2013), we decided to quantify similarities and differences between the climates of North America's northern and southwestern aspen, and to characterize the dominant climatic controls on their distributions. We extended the approach of Rehfeldt et al. (2009) and Worrall et al.

(2013) by creating and comparing ensemble species distribution models (SDMs) for the entire range of aspen, as well as for the northern and southwestern clusters described by Callahan et al. (2013). We also used 10 different statistical modeling methods when creating our ensemble models, as opposed to the single approach used in earlier studies.

2.3 Methods

To better understand climate differences between the northern and southwestern clusters identified by Callahan et al. (2013), we used methods that have been used to measure niche overlap between SDMs (Franklin, 2010, 2013; Warren et al., 2014; Warren et al., 2008). For these analyses, three ensemble distribution models were created: one for the entire population (EP), one for the northern cluster (NC), and one for the southwestern cluster (SC) using 10 different modeling methods (Table 2.1). The NC and SC range boundaries (the grey boundary in Figure 2.1) are adapted from a map of the distributions of the northern and southwestern clusters defined by Callahan et al. (2013) using SSR data. After the creation of the ensemble models, the predicted distributions and climates were compared between EP, NC, and SC.

We used an ensemble modeling approach because it provides more robust estimates of distributions than are possible when using a single type of model (Araujo & New, 2007). Models were built with the biomod2 package (Thuiller et al., 2014) in R (R Core Team, 2014) using a high performance computing cluster at the College of Forestry at Oregon State University. Each final predicted range and climate association was calculated from 200 models derived from 20 runs of 10 model types (Tables 2.1 and 2.2, Appendix S4).

The final models are the averages of all models that met a minimum accuracy of 0.6 measured using the True Skill Statistic (TSS) (Allouche et al., 2006). A value of 1 for TSS represents perfect correspondence between predicted and measured species presences and absences, whereas a value of 0 represents no correspondence. The input presence and absence data (see Appendix S1) were from Worrall et al. (2013) and the climate data (Table 2.2 and Appendix S2) were either taken directly or calculated from the WorldClim dataset (Hijmans et al., 2005). For EP, we used an equal number of presence and absence points, for a total of ~100,000 points. For NC and SC, aspen presences within each region were used in conjunction with all absences across the range of aspen (roughly 94,000 total points for NC, and 53,000 total points for SC, see Table 2.3). We used 80% of the input points for model training and withheld 20% for model testing.

Schoener's statistic, and the modified Hellinger's statistic, D and I were used to evaluate niche overlap (Schoener, 1968; Warren et al., 2008). The D, and I metrics are defined as follows:

$$(1)\ D\left(p_{x.i},\ p_{y.i}\right) = 1\ -\ \frac{1}{2}\sum\left|p_{x.i} - p_{y.i}\right|,$$

$$(2)\ I\left(p_{x.i},\ p_{y.i}\right) = 1 - \frac{1}{2}\sqrt{\sum(\sqrt{p_{x.i}} - \sqrt{p_{y.i}})^2},$$

where $p_{x.i}$ and $p_{y.i}$ are the probabilities of occurrence for species x and y at location i. For D and I, a value of zero indicates no niche overlap, and a value of 1 indicates complete niche overlap.

The relative contributions of each climate variable to each model are also important for understanding why NC, SC, and EP may differ. This was measured by biomod2 using the following methodology. Once a model was trained and run, the model was run a second time with the values of one of the input variables randomized. One minus the correlation between the original prediction (with all the original variables) and the new prediction (with the randomized variable) provided an index of relative importance of the climate variable. A higher relative importance value for a given climate variable indicates greater influence on the modeled species distribution.

2.4 Results

Maps of predicted distributions for the ensemble models EP, NC, and SC are shown in Figure 2.1. The TSS values (i.e., model evaluation metrics) for these three models were 0.868, 0.727, and 0.915, respectively, with all scores indicating good model fit to presence and absence data. EP predicted contiguous aspen habitat in central Canada, the Great Lakes region, the northern Rocky Mountains, pockets in Utah and Colorado, the Sierra Nevada Mountains of California, and isolated areas in Arizona, New Mexico and Mexico. These predictions generally agreed with Little's aspen range maps (Little, 1971) and the predicted distributions described by Rehfeldt et al. (2009) and Worrall et al.

(2013). However, the predicted distributions for NC and SC were very different, and suggested that NC and SC aspens occupy different climates.

To further test the hypothesis that the climate envelopes of NC, SC, and EP were different, we compared D and I among the models. D and I were very low between NC and SC (0.006 and 0.018, respectively), showing that the predicted climate occupancy was different between the northern and southwestern clusters. D and I were also very low between SC and EP (0.037 and 0.089), but D and I between EP and NC were much higher (0.710 and 0.820). These results suggested that SC inhabits a different climate than EP or NC, and that this climate was closer to the edge of aspens' overall climate niche compared to NC. Interestingly, the TSS scores for SC and NC were also higher than for EP.

Because NC and SC were created from different aspen presence datasets, we examined how the climate datasets differed between EP, NC, and SC. Boxplots of the climate variables at the aspen presence points used in each ensemble model are shown in Figure 2.2. The median and interquartile range of SC compared to EP and NC showed that SC had very different AET/MAP, growing degree days (dd5), PET, PET/MAP, precipitation seasonality (psea), temperature minimum (tminyr), and temperature range (trang). The boxplots of the climate variables for EP and NC were more similar. Wilcoxon rank sum tests also showed that the climate variables for SC were statistically different from both EP and NC ($p < 0.0001$). Also, Wilcoxon rank sum tests showed that the climate variables for EP and NC were also statistically different from each other ($p < 0.01679$).

Finally, the climatic ranges of the absence data (which were the same for EP, NC, and SC) extended beyond the ranges of the presence data for EP, NC, and SC (Figure 2.2, Appendix S3).

The relative importance data (Figure 2.3) showed that EP, NC, and SC had climate variables that were similar in importance, ranging between ~0.15 and ~0.35. The biggest exceptions were PET and temperature maximum. PET was much more important in SC (0.83) than in either EP (0.15) or NC (0.31), and temperature maximum was more important in SC (0.41) than in NC (0.13) or EP (0.21). The importance of growing degree days was similar between NC (0.26) and SC (0.30), but less important in EP (0.18). Mean annual precipitation was less important in NC (0.08) than in either EP (0.14) or SC (0.21). The boxplots and Wilcoxon rank sum tests showed differences in PET, temperature maximum, growing degree days and mean annual precipitation between SC and NC. PET and temperature maximum were greater in SC than in NC, and growing degree days and mean annual precipitation were lower in SC than in NC (Figure 2.2). Overall, comparisons of the ensemble models' distributions and climates, the comparisons of D and I, and the relative importance of each climate variable, all suggested that the northern and southwestern clusters occupy different climates.

2.5 Discussion

Our results show that aspens in the northern and southwestern clusters occupy different climates. This is indicated by the large differences in predicted distributions between NC and SC, the small amount of climate overlap (low D and I), the differences in the climates

of the aspen presence points for SC relative to NC and EP, and the dissimilarity in the relative importance of the climate variables to each model. Furthermore, the relative importance of the climate variables showed that PET and growing degree days were more important in NC and SC than EP. In contrast, mean annual precipitation and temperature maximum were more important in SC and EP than in NC. If aspen populations in the EP, NC, and SC clusters responded similarly to climate, we would expect the relative importance of the climate variables to the models to remain the same. Instead, the relative importance of the climate variables differ.

Our overall conclusions are also supported by finer scale studies documenting population differences in adaptive traits that are associated with latitude and climate variables including cold hardiness, and water stress tolerance (Gylander et al., 2012; H. T. Li et al., 2010; Schreiber et al., 2013). In addition, Gray et al. (2011) found associations between growth performance and climate envelopes in western Canada, while Mock et al. (2012) found a potential relationship between the frequency of aspen triploidy and an ombrothermic index (the ratio of the total precipitation sum and mean temperature where temperature mean is greater than zero). Also, our finding that SC occupies a different climate than EP, or NC, is consistent with the hypothesis of Worrall et al. (2013) that aspens in the southwestern United States live on the edge of aspens' overall climate niche.

Our findings rest on three assumptions: The first assumption is that the differences between NC and SC do not result from spatial autocorrelation alone. For example, the

spatial clustering of similar values in climate layers relative to input data presence and absence points could introduce bias to SDM predictions. Secondly, we assumed that differences between the ensemble model results represent biological differences between the clusters and not differences between the model methods that comprise each ensemble (see Appendix S4). However, even if the contributing model methods differ between the ensemble models, we used robust techniques to measure our models' predictive powers and found that TSS was high in each final ensemble model. The final assumption is that the climate occupancy we measured reflects the climatic tolerance or adaptive potential of each cluster. This assumption is well supported by results from regional common garden studies. For example, Gray et al. (2011), characterized growth using common gardens, and climate niche using SDMs, and found that aspen subpopulations in Western Canada were locally adapted to climate. (Gray et al., 2011; Gylander et al., 2012; Schreiber et al., 2013). Broader common garden studies in aspen could be used to further test this hypothesis, but common garden studies have their limitations. Common garden studies do not measure fitness per se, but instead, typically use short-term growth as a surrogate. Furthermore, because they usually use planted seedlings, they do not capture climatic tolerances of many important parts of the life cycle—e.g., flowering, pollination, fertilization, seed production, germination, and seedling establishment or clonal reproduction. Thus, in many respects, SDMs are probably better than common garden experiments for inferring climatic tolerances of naturally regenerated forests. Another advantage of using SDM methods to infer climatic tolerances is that it is possible to study

more populations from a greater geographical area than is possible using common garden tests. For example, we analyzed 97,486 presence and absence locations. Therefore, by using SDMs, we widened the analysis of aspen-climate comparisons.

The regional differences in our SDMs, as well as results from common garden studies from aspen and other forest tree species strongly suggest that NC and SC differ because of evolutionary adaptation to alternative climates. However, other explanations are possible. First, the results of Callahan et al (2013) suggest that the differences we observed may have resulted from geographically distinct, climate-independent, evolutionary pathways. That is, these differences may have been largely random, or driven by selection to climates in the distant past, rather than the recent climates we measured. Second, the geographic differences we observe may be driven by differences in biotic interactions between the regions, rather than differences in adaptation to climate alone (e.g., inter-specific competition or pathogen interactions). However, despite these alternative explanations, it is doubtful that any of these possibilities explain our observations independent of climate impacts because climate is an important constraint to plant distributions (Warren et al., 2008).

Global climate change is expected to transform the distributions of many forest trees (Noss, 2001) and regional or local differences in climatic adaptation are important to consider when predicting the impacts of climate change and designing effective adaptation and mitigation strategies. The differences in the D and I metrics of niche overlap between SC and NC strongly suggest that aspen distribution models should be

tailored to reflect local adaptation to climate. By doing so, we should improve projections of future aspen distributions (or at least potential habitat) and, thus, improve the success of assisted migration. Future range-wide studies in aspen that merge genetic and finer scale SDM approaches will help scientists and natural resource managers to understand species-environment interactions, which will lead to better aspen forest management.

2.6 Figures

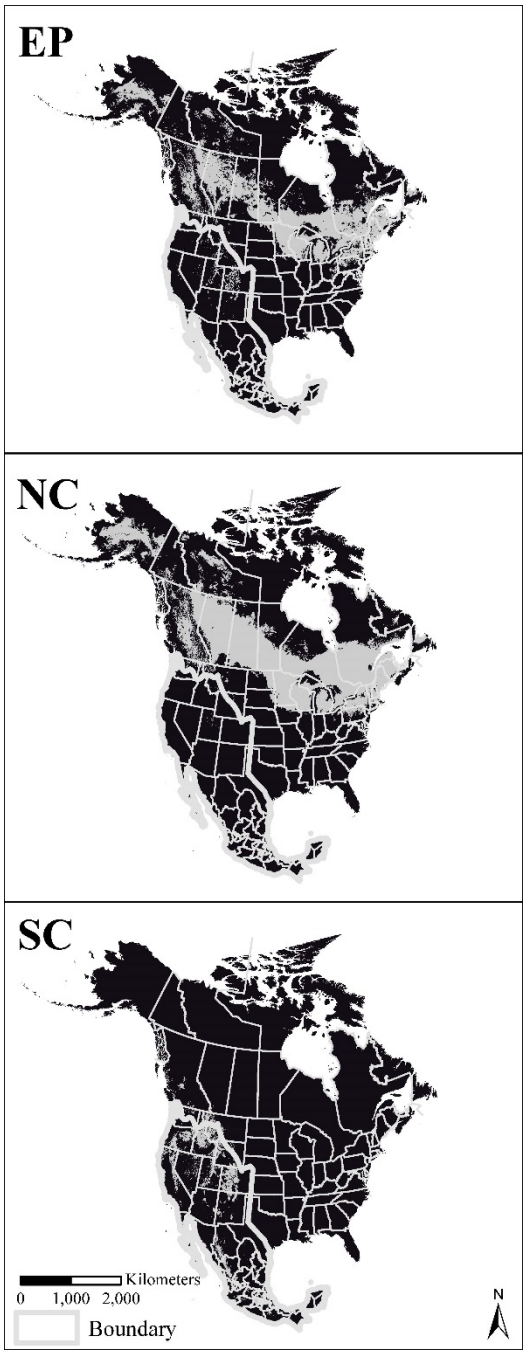

Figure 2.1 Predictive Maps of Aspen's Distribution. The white line is the boundary for the presence data of NC and SC.

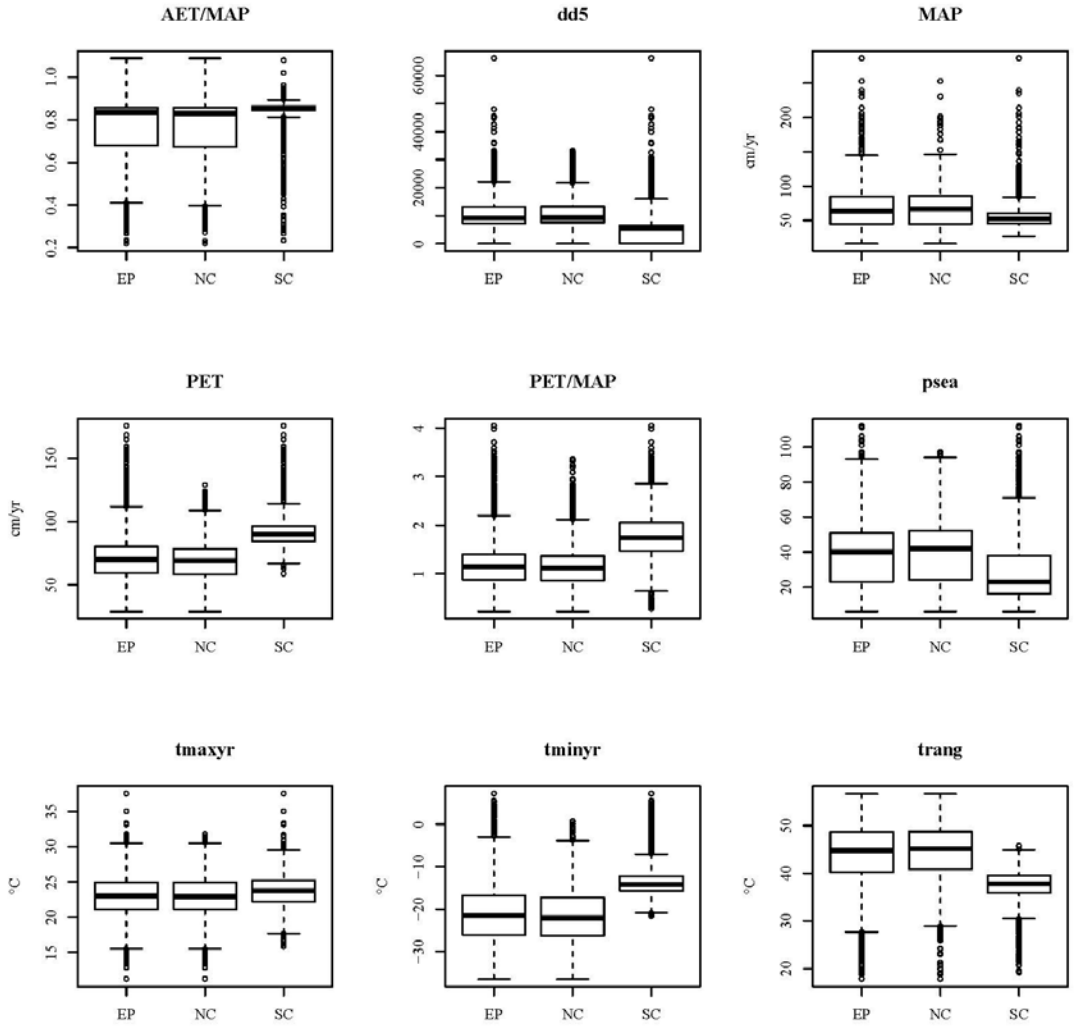

Figure 2.2 Climate variables at aspen presence locations for EP, NC, and SC. Axes without labels are unitless.

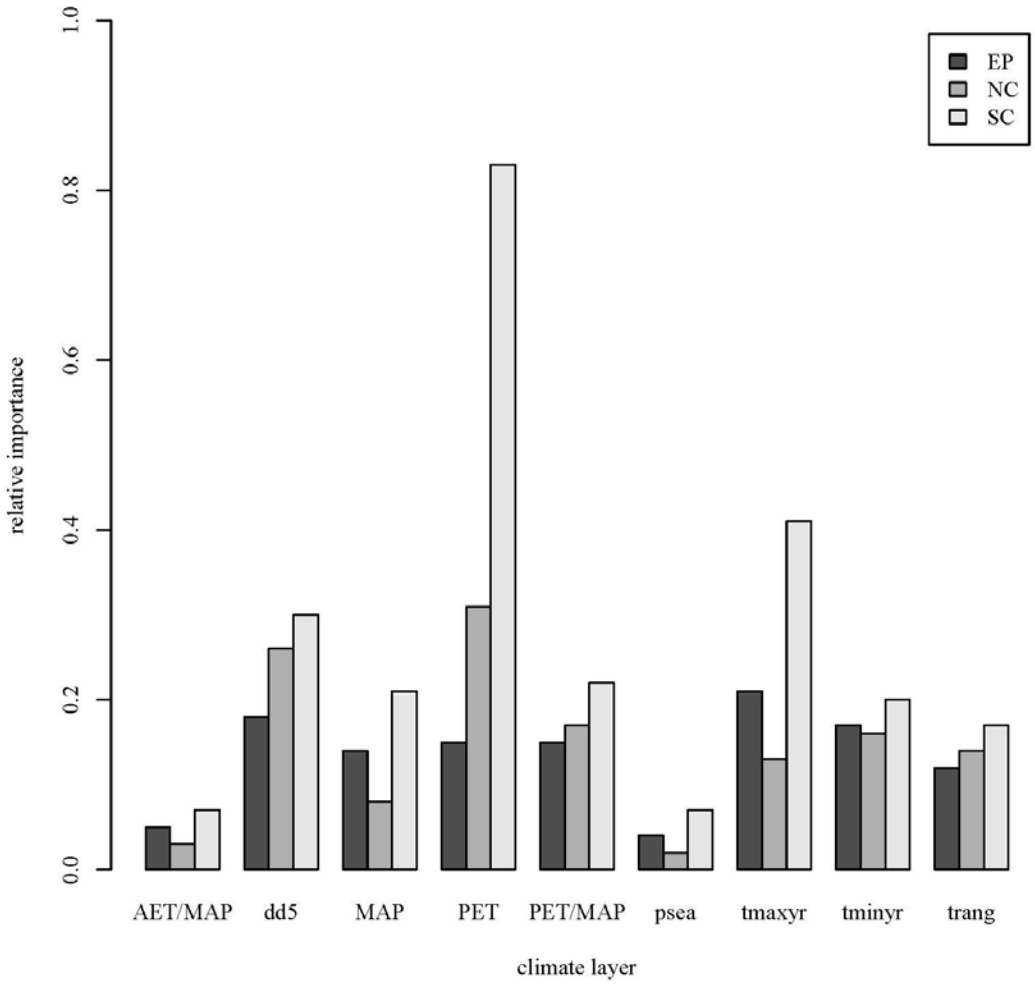

Figure 2.3 Relative importance of each climate layer. Only model runs where TSS was greater than 0.6 were included in the final ensemble model, and each model method varied in the variables important to each model; therefore the variable importance reported are weighted by the actual model contributions to each ensemble model (EP, NC, and SC)

2.7 Tables

Table 2.1 Modeling Methods:

GLM: Generalized Linear Model

GAM: Generalized Additive Model

GBM: Generalized Boosting Model (also known as Boosted Regression Tree)

CTA: Classification Tree Analysis

ANN: Artificial Neural Network

SRE: Surface Range Envelope (BIOCLIM)

FDA: Flexible Discrimination Analysis

MARS: Multiple Adaptive Regression Splines

RF: Random Forests

MAXENT: Maximum Entropy

Table 2.2 Climate Layers used for modeling

Growing Degree Days (dd5), unitless
Mean Annual Precipitation (MAP), mm/yr
Potential Evapotranspiration (PET), mm/yr
PET/MAP, unitless
AET/MAP, unitless
Precipitation Seasonality (Summer Precipitation/Winter Precipitation, or psea)
Temperature Maximum (tmaxyr), °C
Temperature Minimum (tminyr), °C
Temperature Range (trang), °C

Table 2.3 Presence and Absence Data Density

	EP	SC	NC
Total Points	97486	51825	94968
Presence Points	48179	2518	45661
Absence Points	49307	49307	49307
Area Bounding Presence Points (km^2)	21,252,207	4,801,382	16,450,825
Total Density for Area Bounding Presence Points (pts/km^2)	0.0046	0.0108	0.0058
Presence Density per Area Bounding Presence Points	0.0023	0.0005	0.0028
Absence Density per Area Bounding Presence Points	0.0023	0.0103	0.003

3. Polyploidy in Quaking aspen (Populus tremuloides Michx.) influences plant-climate interaction and increases susceptibility to climate-induced drought stress

Summary

- We studied the connection between polyploidy and nearly 40 physiological/morphological traits in a stand of quaking aspen (*Populus tremuloides* Michx.) in the southern Rocky Mountains (USA) that have been subject to widespread mortality from Sudden Aspen Decline (SAD).
- We measured intrinsic water-use efficiency-related traits in five pairs of diploid and triploid clones. We found that triploid aspen had different structural traits including lower stand density, and greater leaf area, leaf mass, leaf mass per area, % Nitrogen content, chlorophyll content, and stomatal size. These trait differences also corresponded to ploidy type differences in plant function where triploids had greater potential net carbon assimilation (*A*, measured using A/C_i curves, and leaf florescence from Rapid Light Curves) and greater stomatal conductance (g_s) than diploids.
- We learned that triploid aspen were less conservative in water loss than diploids. However, triploids also had significantly higher intrinsic water-use efficiency (*iWUE*, calculated from measurements of $\delta^{13}C$ in leaf tissue).
- We suggest that triploid aspen are more sensitive to drought than diploid aspen because they have greater potential water loss because of higher g_s and showed lower stomatal sensitivity to increasing vapor pressure deficit. Therefore, despite

greater *iWUE*, they may have lower resilience in the presence of climate-induced drought stress.

3.1 Introduction

The biogeography of recent and widespread mortality in quaking aspen (*Populus tremuloides* Michx.) overlaps where aspen polyploidy frequency is highest and where aspen grow in warmer and drier climates than most of its range (Callahan et al., 2013; Greer et al., 2016; Mock et al., 2012). This mortality, deemed Sudden Aspen Decline (SAD), followed heat and drought stress in 2002 and 2003 in the western United States and for more than a decade afterwards, SAD-affected clones experienced diminished whole-ramet hydraulic conductance and reduced intrinsic water-use efficiency (L. D. Anderegg et al., 2013; Anderegg et al., 2014; Anderegg et al., 2012; W. R. Anderegg et al., 2013; Huang & Anderegg, 2012; Worrall et al., 2008; Worrall et al., 2010; Worrall et al., 2013). The combined effects of SAD and climate change are driving a massive shift in the composition of some forests in the southwestern United States. In the front range of Colorado, a recent resampling of plots first sampled in 1972-1973 (Peet, 1981) showed that 22 of 89 plots that previously had aspen no longer contain aspen, and where aspen remain, there are fewer aspen in all size classes (Bretfeld et al., 2016). In a separate study near Crested Butte, Colorado (on the western slope of the Central Rocky Mountains), aspen stand density and basal area decreased by 32% between 1964 and 2010, likely in response to both SAD and browsing by ungulates (Coop et al., 2014). Finally, the Pando clone, a triploid and the largest known aspen clone (Mock et al., 2012; Mock et al., 2008)

is also experiencing low regeneration of new suckers, illustrating that for at least this triploid, environmental conditions have not been favorable (Rogers & Gale, 2017). Climate change projections predict that both temperatures and drought stressors will increase in this region and we should expect that aspen in North America will experience SAD again in the future (Worrall et al., 2013). Furthermore, while high frequencies of both diploids and triploids were found in western United States ecosystems and their frequency correlated with precipitation and temperature, it is not yet well established at fine scales how aspen ploidy types interact with climate (Mock et al., 2012). Perhaps, as evidenced in the broader geographical distribution of polyploid aspen, polyploidy confers advantages in warmer and drier climates and as hypothesized in Mock et al. (2012) is a factor in SAD-related aspen forest mortality.

Polyploidy can affect species-environment interactions when the duplicated genomes of polyploid plants alter gene expression to ultimately change phenotypic traits that embody the physiological and mechanistic drivers of plant structure and function (Barker et al., 2016; Madlung & Wendel, 2013; Maherali et al., 2009; Segraves & Anneberg, 2016; Soltis et al., 2014). Recently, these effects were illustrated in 13 separate allopolyploid species (10 ferns and 3 angiosperms), where most polyploids were found to have niche separation from diploids, though the degree of separation depended on the species (Blaine Marchant et al., 2016). Several other studies also illustrate that ploidy types can differentially sort along climate gradients. For example, wild potato (*Solanum* section *Petota*) triploids have been found to live in warmer and drier climates than diploids,

while tetra-, penta- and hexaploids are found in cooler, and wetter places (Hijmans et al., 2007). Also, creosote (*Larrea tridentata*) diploid, tetraploid, and hexaploid ploidy levels align to gradients of summer temperature and precipitation with hexaploids being the most tolerant of hot, dry summers, while diploids are the least tolerant and tetraploids are intermediate (Hunter et al., 2001). A mechanism for climate sorting by ploidy type is that polyploidy modifies functional traits related to drought and heat stress tolerance or avoidance. For example, higher ploidy levels in *Atriplex canescens* have greater resistance to drought-induced loss of stem hydraulic conductivity and thus greater drought resistance (Hao et al., 2013). Furthermore, *Atriplex canescens* ploidy biogeographies also vary relative to soil water availability: hexaploids are most frequent in fine textured soils with low water permeability from which water is more difficult to extract (Dunford, 1984).

Some polyploid trees have greater water-use efficiency than diploid trees of the same species. Water-use efficiency is the ratio of carbon uptake to water loss and is often quantified as intrinsic water-use efficiency (*iWUE*), which is calculated as the ratio of measured net carbon assimilation (*A*) against stomatal conductance (g_s). *iWUE* can also be inferred from measurements of carbon isotope discrimination ($\delta^{13}C$) (G. D. Farquhar et al., 1989; G.D. Farquhar et al., 1982; G. v. Farquhar et al., 1980; Hsiao & Acevedo, 1974; Seibt et al., 2008). Theoretically, by expressing traits that increase net CO_2 assimilation or reduce transpiration, plants can more easily maintain plant water balance that, during drought conditions, might increase plant fitness. For example, *Cakile*

edentula var. *lacustris* plants grown in a dry environment showed selection towards plants with intermediate leaf sizes that also had higher measured water-use efficiency. However, in a wet environment, there was no selection for leaf size or water-use efficiency and plants with larger leaves had greater vegetative biomass, likely because larger leaves provided greater net carbon uptake (Dudley, 1996). *Betula papyrifera* polyploids have been found to express higher water-use efficiency than diploids with leaves of polyploids containing smaller stomata, more stomata per unit leaf area, a thicker epidermis, and increased leaf pubescence, which might increase their resilience to climate stressors like heat and drought. Furthermore, during a 2-hour water stress treatment, *Betula papyrifera* diploids reduced net photosynthesis and stomatal conductance more and maintained less negative water potentials than polyploids (W.-L. Li et al., 1996). These physiological and water-use efficiency related differences between ploidy types in *Betula* also manifest in different ploidy type biogeographies where diploids are more often found in cooler and wetter environments than polyploids.

The biogeographical differences between *Betula papyrifera* ploidy-types are remarkably similar to quaking aspen whose populations living in cooler and wetter northern latitudes are virtually 100% diploid (Mock et al., 2012). Perhaps, in quaking aspen, diploids and polyploids have structural and functional differences similar to *Betula papyrifera*. Polyploids are common in *Populus*, whose current species are thought to have evolved from past polyploids (Sterck et al., 2005). Triploid European aspen (*Populus tremula* L.) have been found to grow faster than their diploid counterparts, likely because triploids

have higher quantum yields of CO_2 fixation, and greater rates of light-saturated net photosynthesis (Pärnik et al., 2014). Presumably, higher net CO_2 assimilation and growth could be beneficial for fast-growing, early successional species like aspen, which have evolved to colonize forest canopy openings after disturbance. If a higher quantum yield in *Populus* triploids also correspond to maintained or reduced transpiration rates, *Populus* triploids would also have higher *iWUE*, a trait that could be advantageous in the warmer and drier southwestern portion of its range.

In stands of co-occurring diploid and triploid aspen, triploids have been found to have greater basal area increments over time (DeRose et al., 2014). However, within aspen stands, other physiological differences between quaking aspen's ploidy types, as well as differences in their ploidy-environment interactions or climate tolerances have not been quantified. Furthermore, we speculate that these factors are important to aspen forest resilience to past and/or future SAD events and climate change. In this study, we examined physiological and drought-tolerance related traits in co-occurring diploid and triploid aspen to understand if diploids and triploids displayed differences in water-use-efficiency-related traits. In a naturally occurring aspen stand in Colorado, we measured clone, ramet and leaf traits, photosynthetic and stomatal conductance rates, and *iWUE* to determine whether polyploidy confers any advantages or disadvantages to aspen occurring in a climate representative of southwestern aspen.

3.2 Methods

3.2.1 Study Site

The study site (38.716 N, 106.819 W) was a naturally occurring aspen stand near the towns of Almont and Crested Butte, Colorado, and the Rocky Mountain Biological Laboratory (in Gothic, Colorado) at 2750 meters in elevation (Figure 3.1). The climate measured at three nearby weather stations (Crested Butte, Gunnison, and Taylor Park) show that the 1980-2014 average May to September temperatures was 11.3°C, and the October to April mean temperature was -5.2°C. Also, the 1980-2014 May to September average total precipitation was 19.1 cm and the October to April average total precipitation was 21.6 cm (Global Historical Climate Network Dataset (GHCN), http://www.ncdc.noaa.gov/cdo-web/).

3.2.2 Study and Statistical Design

We compared physiological and morphological traits in 5 pairs of diploid and triploid clones found throughout the stand (Figure 3.1). One major challenge in studying quaking aspen is that these “trees” are in fact clones, and each clone is made of multiple stems (ramets) that have grown from root suckering (Mitton & Grant, 1996). Individual clones throughout the stand were visually identified and tested for ploidy using flow cytometry (see below for details). Then we selected five diploid and five triploid aspen clones for continued study. Each clone was spatially segregated from other clones of similar ploidy to ensure they were independent clones. Because a single aspen clones actually consists of multiple ramets, we chose to represent an aspen clone using measurements in five

separate (but nearby) ramets in each clone. For each clone, we selected ramets whose bark and leaf color and size were similar and were growing within 20 meters of each other to ensure that each ramet was a member of the same clone. We tested the ploidy of each selected ramet as an extra precaution (details below). We also chose clones of different ploidy in pairs (with similar proximity) to minimize any potential within-site differences driven by geology, and soil type and depth. This paired design allowed us to alternate between clones in a pair for instantaneous measurements that might fluctuate with ambient conditions (see below for details). For our analysis, we used a hierarchical statistical framework where leaf measurements were nested within a ramet, and ramet measurements were nested within each clone.

For our statistical comparisons, we utilized linear mixed models to compare the ploidy types. In each model, the variable of interest was the dependent variable, and ploidy type was the fixed effect. The random effect was set depending on the scale of the measurement: leaf-scale measurements were taken within each clones' ramets, therefore in the mixed models, the clone means for leaf-scale measurements were estimated using a random effect of ramet nested within clone. For ramet-scale measurements, clone identity was the random effect. We fit models using restricted maximum likelihood (REML), ensuring that model assumptions were met, and that residuals were evenly distributed. If residuals showed any patterns (including uneven spread over the fitted values), we adjusted the model to allow residuals to differ between groups, or by trying alternative correlation structures to improve the model fit (see Appendix S7). To evaluate if the

means of our measurements differed by ploidy type, we compared the means using F-tests of overall significance, using thresholds of $p < 0.05$, and $p < 0.10$.

3.2.3 Ploidy Identification

Before choosing clones for our study, we tested the ploidy of multiple clones at our study site using flow cytometry. We used similar methods to the protocol found in Mock et al. (2012) to identify diploid (2n = 2x = 38) and triploid (2n = 3x = 57) clones. Briefly, fresh leaf samples were dried using silica gel (Activa Flower Drying Art Silica Gel) and from each dried sample, 1 cm^2 sized sections were chopped with equally sized fresh samples of diploid *Hordeum vulgare* (1C genome size is 5.55 pg (Bennett & Leitch, 2012)). Nuclei were suspended and stained using the CyStain® PI Absolute T kit produced by Partec. For nuclei extraction, 150 ul of extraction buffer (with 2% by volume polyvinylpyrrolidone) was added to the chopped leaf material. Then, the suspension was filtered using Partec CellTrics disposable tube top filters and 750 ul of CyStain® was added. Filtrates were analyzed using an Accuri C6 (BD, Franklin Lakes, NJ) and excited using a 585 nm laser. Boxplots of the ratios of the median peak florescence of each aspen sample relative to the *H. vulgare* peak florescence were used to determine the ploidy of each ramet (Figure 3.2). Triploid aspen, having an extra set of chromosomes, should have 50% more florescence than diploids, and we assigned ploidy accordingly. In addition, we also tested the ploidy of several samples provided by K. Mock (Utah State University) with known ploidy and found 100% correspondence between ploidy determinations.

3.2.4 Clone, Ramet and Leaf Characteristics

Characteristics of each clone, its ramets and their leaves were measured. First, aspen clone structure, a determinant of the degree of water and light resource competition between ramets, was measured in July of 2014 and July of 2015. Clone basal area per ground area and canopy openness (percent open sky) was measured once per clone using a wedge prism, and a spherical densiometer, respectively.

To capture characteristics of the ramets, we measured diameter at 1.3 meters above ground elevation (DBH) in five ramets of each clone. Each ramet's height was also measured using a laser range finder. Leaf area index (LAI) of four ramets in each clone were measured using a LAI-2000 (LI-COR Biosciences) between first light and dawn. Because clone canopy openness was heterogeneous, LAI measurements were taken for each ramet by averaging LAI measured across four equally spaced measurements (separated by 90 degrees around the ramet) 1.3 meters above ground, and 3 meters away from the stem using the 50% lens cover with the open portion facing the aspen stem. Within each ramet, leaf area was measured on at least ten fresh and healthy, sunlit, leaves from the lower crown by using ImageJ on digital scans of these leaves (Schneider et al., 2012). Oven-dried mass of healthy leaves was also measured in the leaves used for leaf area. Leaf area and mass were averaged by ramet. Leaf mass per area (LMA) was also calculated as dry leaf mass normalized by leaf area. In addition, leaf stomatal sizes (measured as the length of the stomatal guard cells) and densities were measured using a digital microscope (VHX-1000E, KEYENCE CORPORATION) in leaf peels that were

collected in the field. Leaf peels were created by coating the abaxial surface with fast-drying nail polish, and allowing the nail polish to set for ten minutes. We then removed the nail polish using clear tape, and immediately affixed the leaf peel to clear slides.

3.2.5 Photosynthetic Rates and Chlorophyll Fluorescence

We measured the photosynthetic properties of leaves in diploid and triploid aspen. Because photosynthetic rates are modulated by environmental conditions, measurements were alternated between diploid and triploid ramets from paired diploid and triploid clones over a single day (between 09:00 and 14:00), and captured over 5 separate days to characterize all 5 clone pairs. In July of 2015, the relative chlorophyll content of aspen leaves was estimated using a SPAD meter (Spectrum Technologies, Aurora, IL) as the average SPAD of 20 leaves for each ramet. A SPAD meter measures leaf transmittance of red (650 nm) and infrared (940) light and produces a unitless SPAD measurement as an estimate of "greenness" (Ling et al., 2011). We measured A/C_i curves (net CO_2 assimilation rate, A, versus calculated substomatal CO_2 concentration, C_i) and chlorophyll fluorescence to examine photosynthetic efficiency and maximums in diploid and triploid aspen. For *A/Ci* measurements, we used an integrated chlorophyll fluorimeter and gas exchange unit (i*FL*, Opti-sciences Inc, and ADC BioScientific Limited) with a broad-leaf chamber. During June of 2016, we measured 3 leaves on 3 different ramets, again alternating between clone pairs during the measurements. *A* was measured in the leaf chamber where we sequentially controlled the CO_2 concentration of air between 50 and 1600 ppm. Before taking measurements, the leaf was allowed to stabilize to ambient

chamber conditions for photosynthetically photon flux density (PPFD), temperature and CO_2. Afterwards, chamber conditions were set with PPFD at 1500 μmol m^2s^{-1}, the chamber temperature at 25°C, the humidity of the air at 15 mmol of H_2O and the mass flow of air per m^2 of leaf area at 200 (mol m^{-2} s^{-1}). Then CO_2 concentrations were sequentially adjusted to 400, 300, 200, 100, 50, 200, 400, 600, 800, 1000, 1200, and 1600 ppm after measurements of each chamber CO_2 concentration and ΔCO_2 stabilized between steps. At each step, *A* (μmol m^2s^{-1}) was measured, and C_i was calculated (see Appendix S5 for more details on C_i calculations).

The resulting A/C_i curves were fit to the data using the 'plantecophys' R package using the data points collected where CO_2 concentrations increased from 50 ppm to 1600 ppm. Curves were fit using the 'default' method, without temperature correction (the chamber temperature maintained at 25°C for each curve). Curve fitting followed the *A/Ci* model (G. v. Farquhar et al., 1980; P. Harley et al., 1992; P. C. Harley & Sharkey, 1991; Sharkey, 1985) where the carboxylation rate during photosynthesis is limited by: 1) the maximum rate of Rubisco-catalyzed carboxylation (termed "Rubisco-limited", V_{cmax}), 2) the regeneration of ribulose biophosphate (RuBP, or J_{max}) which is regulated by the electron transport rate, J, and 3) the regeneration of RuBP as controlled by the rate of triose-phosphate utilization (TPU). Dark respiration in the light (R_d), the compensation point between Vcmax and Jmax limitations (Γ^*), and K_m (half of the rate at which CO_2 update is maximized) were also compared between ploidy types.

Leaf florescence, an indicator of PSII capacity and efficiency, was measured as using a MINI-PAM (Walz, Effeltrich, Germany). These measurements provided the quantum yield of photosystem II (Φ_{PSII}) and the electron transport rate (J) of diploid and triploid aspen (see Appendix S5 for more details) calculated from background fluorescence (F_t) and maximum fluorescence (F'_m). The maximum quantum yield of PSII (Φ_{PSII}) in the light was calculated as:

$$\Phi_{PSII} = (F'_m - F_t)/F'_m$$

In dark-adapted leaves Φ_{PSII} can estimate the maximum potential quantum efficiency because in dark conditions photosystem II reaction centers should all be 'open'. Φ_{PSII} in dark-adapted leaves is also an indicator of plant photosynthetic performance and can indicate plant stress (Maxwell & Johnson, 2000). Φ_{PSII} can also be utilized to estimate the electron transport rate (J) and therefore overall photosynthetic capacity *in vivo*:

$$J = \Phi_{PSII} * PFDa * 0.5$$

where PFDa is absorbed light and 0.5 is a factor representing the partitioning of energy between photosystem I and photosystem II. Rapid light curves (RLCs) are successive measurements of Φ_{PSII} under increasing quantities of actinic light, and the initial slopes and maximum yields of both Φ_{PSII} and J from RLCs provided useful information about the efficiency of photosystem II, electron transport, and the maximum light that a leaf can use to drive photosynthesis.

In our study, both the maximum quantum yield of PSII in the dark and RLCs in the light were measured. During July of 2015, between the hours of 03:00 and 05:00, twenty

measurements per ramet of F_0 and F_m were collected in the dark. In July of 2015 and June of 2016, during ambient lighting conditions between 10:00 and 14:00, RLCs were measured in three sunlit leaves in each of the 50 ramets. RLCs were alternated between paired diploid and triploid clones over 5 days. During sunlit conditions, the RLC leaves were shaded at the beginning of each RLC so that RLC could take measurements at where photosynthetically active radiation (PAR) was less than the ambient lighting conditions (whose sunny day maximum was generally between 1800 and 2200 μmol m^{-2} s^{-1}). The minimum and maximum fluorescence (F_t and F'_m) were measured at eight different light levels following a saturating pulse.

Curves were fit to each RLC measurements of Φ_{PSII} (measured in daytime RLCs) using non-ordinary least squares based on equation 2 from (Thornley) that estimates the quantum yield of photosynthesis and the maximum light-saturated photosynthetic rate:

$$\Phi_{\mathrm{PSII}}(I_L) = \frac{1}{2\xi}\left(\alpha I_L + ETR_{max} - \sqrt{[(\alpha I_L + ETR_{max})^2 - 4\xi\alpha I_L ETR_{max}]}\right)$$

We estimated two parameters of this equation: α, the electron transport efficiency (or the initial slope of the $\Phi_{PSII}(I_L)$ curve), and ETR_{max} (the light-saturated photosynthetic rate). I_L was the incident PAR (μmol PAR $m^{-2}s^{-1}$) during the RLC. ξ is the sharpness of the 'knee' of the curve and was set to 0.9. We estimated α and ETR_{max} using the nls2 package in R using the least squares method. During our statistical tests, we tested for significant differences for the $\log(\Phi_{PSII})$ between the ploidy types for the combined data, and for differences in α and ETR_{max} derived from individual RLCs.

3.2.6 Stomatal Conductance

Stomatal conductance (g_s) was measured in both clones in July of 2014, and again in June and July of 2015 using a SC-1 leaf porometer (Decagon Devices Inc.) in three sunlit leaves per ramet on the abaxial surface of each leaf. Because vapor pressure deficit (*D*) can drive changes in g_s (Collatz et al., 1991; Hogg & Hurdle, 1997; Jarvis, 1976), we also calculated *D* from measured temperature and relative humidity at a nearby weather station near Almont, Colorado (38° 39' 17" N, 106° 51' 42" W, 2500 meters in elevation) operated by the Rocky Mountain Biological Laboratory. *D* for each g_s measurement was matched from the closest climate measurement to observations in time. Climate station measurements were recorded every hour in 2014 and every 10 minutes in 2015.

3.2.7 Leaf Specific Hydraulic Conductivity

In June of 2016, we measured the hydraulic conductivity (K_h) of small branches in diploid and triploid aspen. Like many of the previous measurements, K_h measurements were paired between diploid and a triploid clones over 5 days. We took one terminal branch segment from 4 different ramets in each diploid and triploid clone (with 40 total measurements across all clones). The branch segments (5 mm diameter and 5 cm length) were clipped from the lower sunlit canopy, and immediately placed in a water-filled tube. Just prior to the measurement, the branch was removed from the water tube while underwater in a deep dish, submerged for 15 minutes, and then recut. Afterwards, the bark was peeled from around both ends of the segment. We then measured K_h using a high pressure flow meter (Tyree et al., 1995), recording our final measurements when the

difference between upstream and downstream pressures were stable for 15 minutes (the mean difference in pressure was 3.8x10-^{2} MPa). We corrected all measurements to 20°C equivalent measurements because temperature can affect the viscosity of water and thus the raw measurements of K_h. Afterwards, we normalized K_h by xylem cross-sectional area (K_s) and by leaf area distal to the branch segment (K_l) using measurements of cross-sectional area of the segment and leaf area distal to each segment.

3.2.8 Intrinsic Water-use Efficiency

Intrinsic water-use efficiency (*iWUE*), the ratio of *A* to g_s, was calculated from measurements of carbon isotope ratios, $\delta^{13}C$, from leaf tissue. *iWUE*, was calculated using $\delta^{13}C$, atmospheric [CO_2], C_a, and intercellular [CO_2], C_i (Seibt et al., 2008) where *iWUE* was defined as:

$$iWUE = \frac{A}{g_s} = \frac{(C_a - C_i)}{1.6},.$$

And, following the model of G.D. Farquhar et al. (1982), C_i was derived from measurements of $\delta^{13}C$:

$$\delta^{13}C = \delta^{13}C_a - a - (b - a)(\frac{C_i}{C_a}),$$

where, $\delta^{13}C_a$ is the carbon isotope ratio in the atmosphere, *a* is the fractionation against $^{13}CO_2$ during molecular diffusion through the stomata (~4.4‰), and *b* is net fractionation due to carboxylation by the Rubisco enzyme (-27‰). We measured $\delta^{13}C$ in aspen leaf tissue, and derived C_i and *iWUE* using the above equations, using the mean June and July 2014 $\delta^{13}C_a$ and C_a of air measured at Niwot Ridge, Colorado (White & Vaughn, 2011). $\delta^{13}C$ was measured in pooled samples of ground leaf material from each ramet, using

continuous-flow isotope ratio mass spectrometry (samples were combusted in a Carlo Erba elemental analyzer and isotope-ratios and % mass were measured using a Thermo DeltaPlus isotope ratio mass spectrometer) at Oregon State University's Stable Isotope lab in Corvallis, Oregon. We also measured %N and %C in these leaf samples. %N is an important metric because %N scales linearly with *A (Evans, 1989)*. Standard errors of 11 replicates for the measurements of $\delta^{13}C$, %N, and %C were +/- 0.2 ‰, 0.1%, and 0.1%, respectively.

3.3 Results

3.3.1 Physiology

At the clone scale (Table 3.1), we found that the basal area per unit ground area was significantly greater in diploid stands (17.53 m^2 ha^{-1}) than in triploid stands (11.37 m^2 ha^{-1}). However, the mean DBH (10.9 cm) and height (5.0 m) of the ramets did not differ between ploidy levels. Using the mean DBH, and the mean basal area per unit ground area, we also calculated that, on average, diploid clones had 1914 trees per ha, and triploid aspen had 1188 trees per ha which equates to triploid aspen clones having 62% of the number of trees found in diploids. Open canopy percentage was also similar between ploidy types (mean = 28% open).

We identified several leaf traits that differed between the ploidy types (Tables 1 and 2). Triploids' leaves were nearly twice as large as diploids' with 76% greater overall dry mass and slightly (12%) greater LMA. SPAD was also 28% greater in triploids than in diploids. LAI and the leaf areas distal to the segments used for measurements of K_l and

K_s were similar across ploidy levels and because diploids had smaller leaves, triploids likely also had fewer leaves. Stomata were also 35% longer in triploids than in diploids. Leaf stomatal density was not statistically different between ploidy types ($p < 0.50$). We used the mean stomatal length measurements to predict diploid and triploid stomatal area and average stomatal area per leaf: assuming that each stomata was an ellipse and that its width was half of the length, the mean area per stomate for triploids was nearly twice that of diploids (1742 μm^2 and 958 μm^2, respectively). By combining leaf size of diploids and triploids (13.4 cm^2 and 21.1 cm^2, respectively), with their stomatal areas, the average total stomatal area per leaf for triploids was approximately three times that for a diploid leaf (diploids = 0.68 cm^2 and triploids = 1.85 cm^2). Remembering that LAI was not statistically significantly different between ploidy levels, it suggests that for the same leaf area, the total stomata area per ramet for triploids was greater. These findings illustrate a tradeoff between leaf size and number on each ramet – diploid and triploids converged on a similar total leaf area per ramet, but triploids had a greater total stomatal area.

We observed a trend towards higher g_s in triploids, although this difference did not reach statistical significance at the $p < 0.05$ level ($p < 0.07$, diploids = 400 mmol m^{-2} sec^{-1} and triploids = 454 mmol m^{-2} sec^{-1}). When the log of vapor pressure deficit (D) was included in the linear mixed model as a fixed effect (per Oren et al. (1999)), the mixed model predicted that D was important to ploidy level differences in stomatal conductance ($p< 0.01$, Figure 3.3). At high D, triploid aspen had higher stomatal conductance than diploid aspen, but at low D, diploid and triploid aspen had similar stomatal conductance values.

Diploids were also more sensitive to increasing *D*, as indicated by a greater slope ($\frac{g_s}{logD}$) than triploids. Interestingly, K_s and K_l were similar between the ploidy types, though triploids trended higher in each measurement and it is possible that with greater sample numbers, K_s and K_l would be significantly different between diploids and triploids (see Appendix S6, Figure 7.2). Also, similar to the LAI data, the leaf areas distal to each segment were alike between the ploidy types (mean = 415 cm^2).

3.3.2 Photosynthetic Rates and Chlorophyll Fluorescence

As previously discussed, chlorophyll content (measured as SPAD) was significantly different between ploidy levels (Table 3.2). Therefore, we anticipated that our measurements of photosynthetic rates and fluorescence would also show ploidy type differences (see Table 3.3). Indeed, J_{max} trended higher in triploids and was almost statistically different at the $p < 0.10$ level ($p < 0.102$, diploid mean = 129.04, triploid mean = 144.98). However, V_{cmax}, $R_{d,}$ Γ*, and K_m were not significantly different between ploidy types (mean = 69.15, 2.39, 49.42, and 912.55 respectively).

Φ_{PSII} in dark-adapted leaves (an indicator of plant stress) was similar between ploidy levels ($p < 0.32$) with a mean across all diploid and triploid clones of 0.88 (which is 5% higher than the normally estimated 0.84 for dark Φ_{PSII} across all plants). The similarity of Φ_{PSII} in dark-adapted leaves indicates that any differences between ploidy types were likely not driven by differences in plant stress during the measurement period. In addition, we found that $\log(\Phi_{PSII})$ in the light that depended on both ploidy type and PAR ($p < 0.001$, Figure 3.4). From our mixed model we found that the slope ($\frac{\log(\Phi_{PSII})}{PAR}$)

of diploids was greater (more negative) than triploids, suggesting that the quantum efficiency of diploids was lower than triploids. In addition, triploids had a higher maximum quantum efficiency at high light suggesting they had more 'open' reaction centers than diploids at high light, possibly because they had more chlorophyll. We also fit a linear mixed model to J, but did not find that there were statistically significant differences between ploidy types.

We compared the individual RLCs' α and ETR_{max} estimated from fitting equation 2 from Thornley (2002) to each individual light curve measured in 2015 and 2016. The results were not statistically significantly different between the ploidy types for 2015, but were almost statistically significant at the $p < 0.05$ level in 2016 ($p < 0.0572$, triploids were 41% greater) for a subset of 3 diploid-triploid pairs sampled opportunistically while taking *A/Ci* curves.

3.3.3 iWUE

$\delta^{13}C$, and calculated C_i, C_i/C_a, and *iWUE* were all statistically different between diploid and triploid aspen (Table 3.4), with triploid aspen having 12% greater intrinsic water-use efficiency. Percent nitrogen content was also 8% greater in triploids than in diploids ($p < 0.056$) which strongly suggests that triploid aspen have a higher photosynthetic rate. A higher nitrogen content in triploids also corresponded to measured greater chlorophyll content (SPAD), J_{max}, and $\log(\Phi_{PSII})$ in triploids. We also compared %C with %N and found that the C:N ratio in triploids was 9% lower than diploids. Using our leaf measurements, and our measurements of nitrogen content, we calculated several other

metrics of nitrogen in aspen (Table 3.5). We found that the average mass of leaf nitrogen per leaf area was 20% greater in triploids than diploids (calculated by multiplying LMA times %N per mass, 162.78 mmol m^{-2} and 198.48 mmol m^{-2} for diploids and triploids respectively). In addition, the total average mass of nitrogen per leaf was 91% greater in triploids (calculated by multiplying the average mass of leaf nitrogen per area times the leaf area, 0.22 mmol and 0.42 mmol respectively). And the mass of leaf nitrogen per ground area is 5% greater in triploids (calculated by multiplying average mass of leaf nitrogen per leaf area times LAI, 127.08 mmol m^{-2} and 133.51 mmol m^{-2}, respectively).

3.4 Discussion

Our study illustrates that diploid and triploid aspen trees have differences in physiology and function. Many of these differences were obvious in the field: diploids had a higher density of the ramets in the clones, while triploid leaves were greener with larger leaves (Figure 3.5). Our measurements confirmed these field observations where diploids had smaller leaves with less chlorophyll, lower LMA, and a corresponding lower leaf %N, J_{max}, Φ_{PSII}, and g_s. We also found that *iWUE*, calculated from $\delta^{13}C$ was also lower in diploid leaves.

The stand density in diploids, and similarities in LAI, tree height, and canopy openness suggest some interesting trade-offs in canopy structure between diploid and triploid aspen. We found that triploid aspen had 38% fewer trees per ha and triploid ramets had 57% larger leaves with 12% greater LMA. Furthermore, diploids and triploid clones also had similar LAI, tree height, and canopy openness. Together, this could mean that diploid

crowns or canopies may also be deeper or longer. This difference in canopy structure could be expected if larger triploid leaves with greater chlorophyll content and higher LMA required a greater minimum amount of light to maintain canopy light-use efficiency and to have a net positive carbon balance for leaves lower in the canopy (Bonan, 2002; Ellsworth & Reich, 1993). It has been shown that quaking aspen leaf flutter increased lightflecks within the canopy, and subsequently increased CO_2 fixation (Roden & Pearcy, 1993c) and the differences in leaf sizes between diploids and triploids likely also change the size and frequency of these lightflecks in the canopy.

The differences in g_s and *iWUE* between the ploidy types were likely driven by differences in leaf structure. Stomatal size is known to affect g_s where at high *D*, leaves with larger stomata should also have higher g_s than leaves with smaller stomata, and leaves with smaller stomata should have greater control over g_s (Drake et al., 2013; Franks et al., 2009; Lawson & Blatt, 2014; Oren et al., 1999). We found that stomatal size and g_s were also related in aspen: diploids with smaller stomata had lower overall g_s, lower g_s at high *D*, and greater sensitivity to increasing *D* (a more negative slope, $\frac{g_s}{D}$). Conversely, triploid leaves with larger stomata maintained higher g_s than diploids at high *D*. Remembering that boundary layer conductance also affects maximum transpiration, and is mediated by leaf size and wind speed, we considered that the larger leaves in triploids might decrease boundary layer conductance, and therefore transpiration rates (Bonan, 2002; Collatz et al., 1991; Martin et al., 1999 1995; Nobel, 1999). However, trembling leaves in quaking aspen complicate estimates of boundary layer conductance

because, while the trembling motion could increase boundary layer conductance, leaf flutter also reduces leaf temperature, which might instead reduce boundary layer conductance. In fact, it is possible that the flutter rate of aspen leaves, which is driven by factors like leaf size, and canopy structure, could be a greater control to boundary layer conductance than leaf size alone, but we did not measure these factors in this study (Roden, 2003; Roden & Pearcy, 1993a, 1993b, 1993c). We also considered that triploids could reduce total transpiration per ramet by having lower total leaf area per ramet (total ramet transpiration = transpiration per leaf area times total ramet leaf area), but leaf area per ramet was similar between ploidy types. Therefore, if we assume that boundary layer conductance is the same between the ploidy types because of leaf flutter, we conclude that transpiration rates are also cumulatively higher in triploid ramets. Potentially, this also explains why we also found that stem density and the average number of trees per ha were lower in triploids: by having fewer ramets per ground area, triploid ramets could have greater root to shoot ratios than diploid ramets (which could increase the ground water resources allocated to each ramet). It is, however, important to remember that aspen clones commonly share roots with surrounding ramets, though it is unknown to what degree water resources are shared within a clone.

Interestingly, despite triploids having higher g_s rates (and speculating that they have higher ramet scale transpiration), we found that *iWUE* was also greater in triploids, which, in conjunction with our measurements of leaf N, J_{max} and Φ_{PSII}, supports that triploid ramets also have greater CO_2 assimilation rates than diploids. Greater *iWUE*

driven by higher *A* relative to g_s is similar to findings in *Eucalyptus grandis* where increased *A* (driven by nitrogen fertilization treatments) in the absence of a corresponding change in g_s, resulted in lower $\delta^{13}C$ and higher *iWUE* (Clearwater & Meinzer, 2001). However, we might expect that plants that were more heat and drought tolerant might instead increase *iWUE* by decreasing g_s more relative to *A* instead of increasing *A* more relative to g_s. For example, it was found that in apple trees, while *A* measured in 'Fuji' and 'Braeburn' apple tree varietals were similar, g_s was lower and *iWUE* was greater in 'Braeburn' which are more water conserving (Massonnet et al., 2007). In aspen, the photosynthetic and *iWUE* data also suggest greater potential growth in triploid ramets, which could be the mechanism for why triploid clones have higher basal area increments than diploids (DeRose et al., 2014).

From a biogeographical perspective, our findings provide some insight to the understanding of why triploid aspen are more often found in regions that are warmer and drier than the rest of the range (Mock et al., 2012). Triploids are less conservative with water use at high *D*, which provides a carbon uptake advantage to triploids when climatic conditions are not too extreme. Furthermore, a carbon advantage in triploids could potentially allow them to spread over larger areas that diploids (Mock et al., 2012; Mock et al., 2008), which would allow triploids to outcompete diploids as they seek water resources in the mountainous topographically heterogeneous landscapes of the American West. However, during a severe drought (like 2002 and 2003), we reason that triploid aspen ramets would die faster than the more water conservative diploids. There is

insufficient data to confirm or deny these hypotheses, but maps of clone boundaries in stands that experienced SAD, and the ploidy identity of both SAD-affected and healthy clones could illustrate differences between ploidy levels in tradeoffs between growth and water loss. Furthermore, knowing the size and distributions of diploid and triploid clones over larger areas than those that have been studied, and knowing ramet density and changes to clone boundaries over time could aid in untangling the evolutionary ecology of the ploidy types in this species, and how climate change will impact diploid and triploid aspen. Projections of a warmer and drier climate suggest that SAD will continue in the future (Worrall et al., 2013). Given the structural and functional differences between the ploidy types, and that triploid aspen clones are likely sterile and unable to recolonize over long distances as quickly as wind dispersed diploid aspen clones, we might also expect that triploid aspen will be affected by climate change sooner and at faster rates than diploids.

Forest and land-use management plans, or assisted migration proposals, do not often discuss polyploidy in plants. This may be simply because ploidy measurements are not routine, or because the ecological consequences of intraspecific variation in polyploid biogeographies are considered inconsequential compared to interspecific ecological drivers. However, biological and functional differences between diploid and triploid aspen increase the biodiversity of aspen as species, whose forests range across much of North America. Furthermore, polyploid aspen have differences in their physiology and function than diploids that may make them more vulnerable to climate change. We

believe that both diploid and triploid aspen should be maintained in populations because they add to niche differentiation in aspen. Therefore, we strongly recommend that aspen forest management or assisted migration plans consider that aspen polyploids have different climatic requirements than diploids, and require separate management considerations and goals than diploid aspen.

3.5 Figures

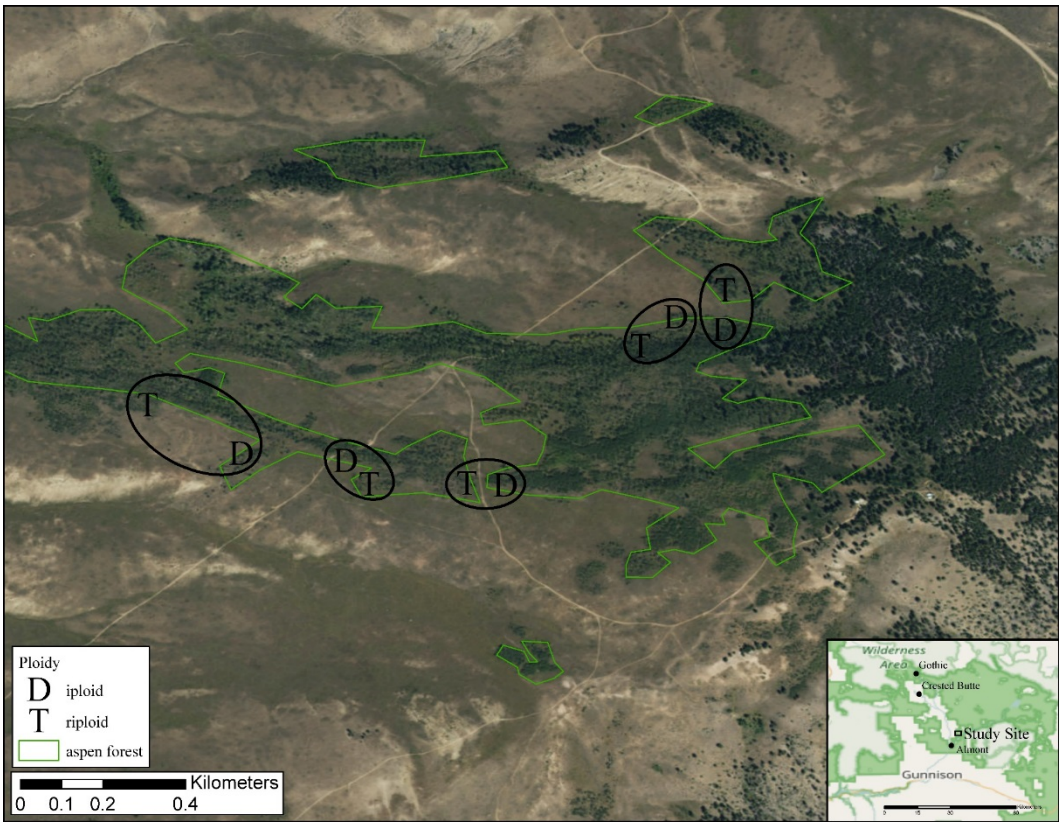

Figure 3.1 The study site and the aspen forest surrounding the studied clones. The circles show the locations of paired diploid (D) and triploid (T) clones

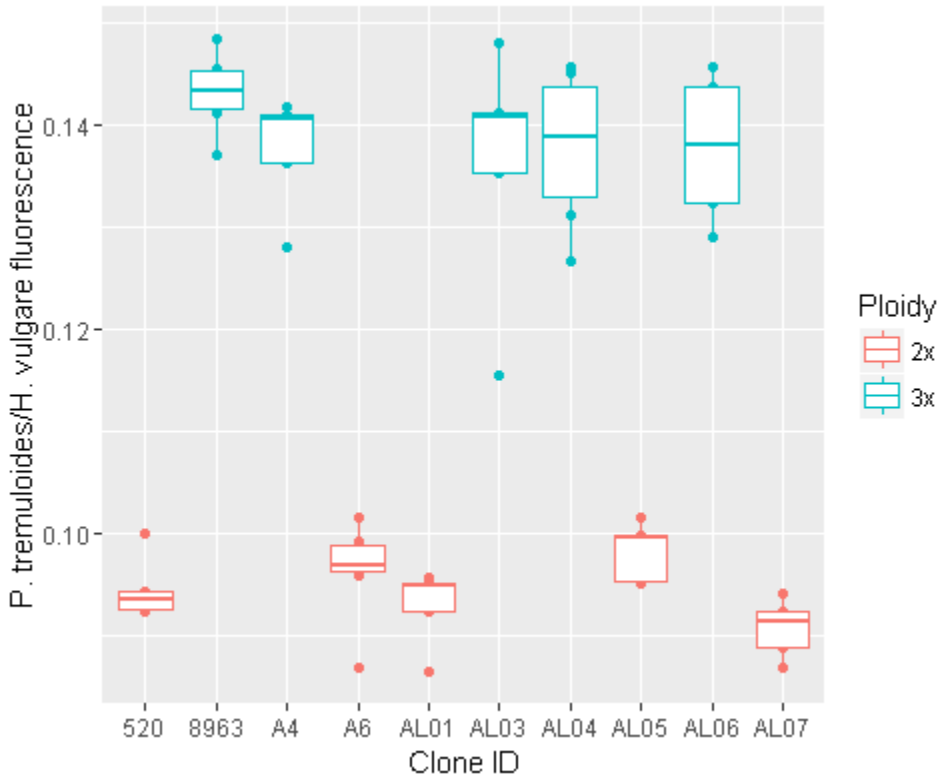

Figure 3.2 The ratios of the median peak florescence intensity of quaking aspen against barley measured in leaves in each ramet of each clone. Triploid aspen were expected to have a brightness that is 50% greater than that of diploid aspen because, containing one extra copy of their chromosomes, they have would 50% more nuclear genetic material than a diploid.

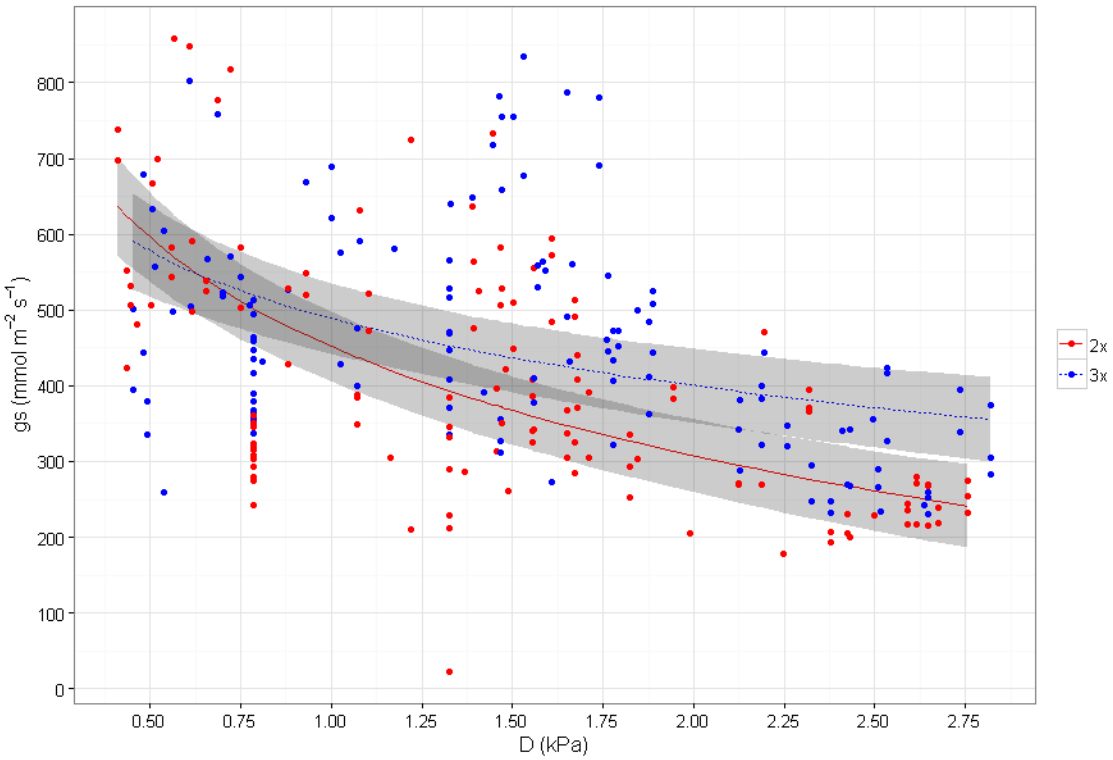

Figure 3.3 Stomatal conductance (g_s) as a function of vapor pressure deficit (D). The lines represent the predicted gs as a function of D from the mixed model and the grey boxes represent standard errors around predictions.

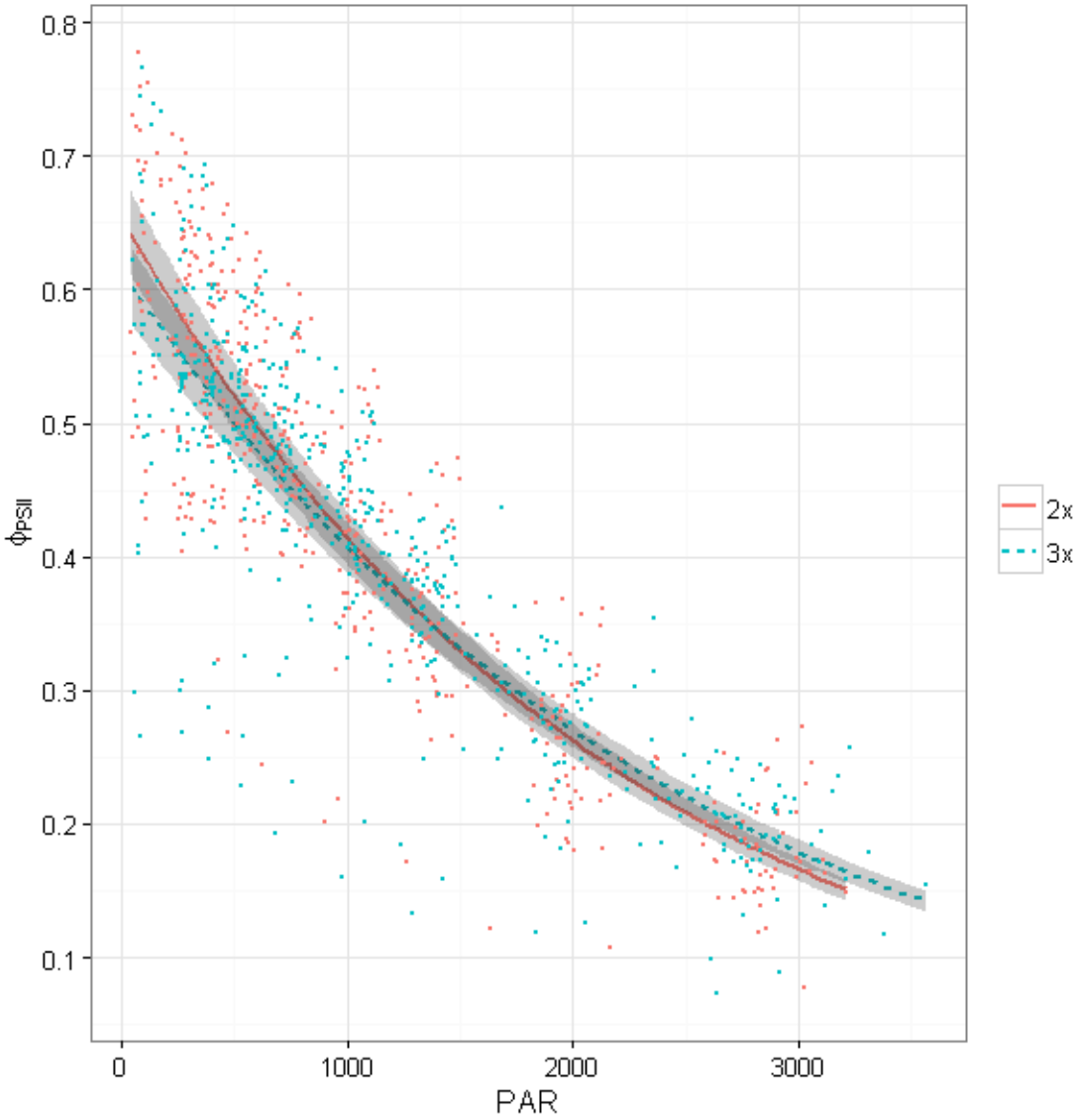

Figure 3.4 ΦPSII as a function of PAR for diploid and triploid aspen measured in RLCs. The lines represent diploid and triploid predictions of ΦPSII relative to PAR and the grey boxes represent standard errors around the predictions.

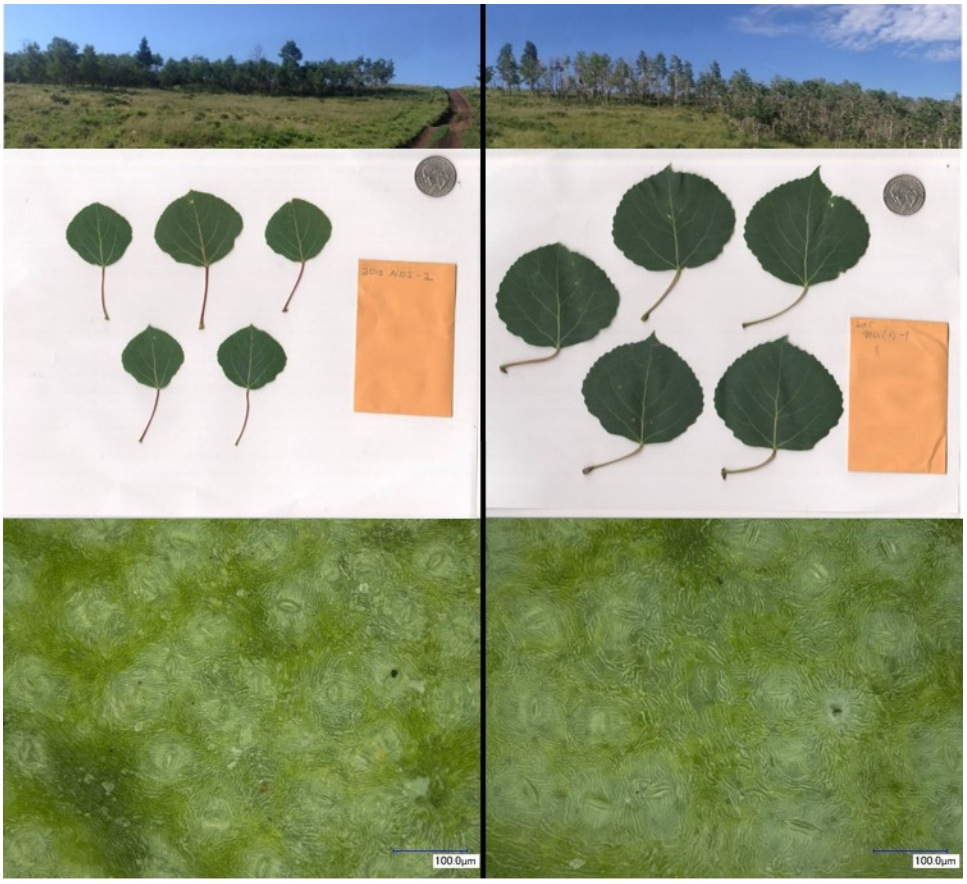

Figure 3.5 Images from two adjacent clones in the Almont site show clear differences between Diploid (left) and triploid (right) traits. Stand density (top), leaf size (middle), and stomatal size (bottom) were all statistically different between ploidy types. Scale bar in bottom row images is 100 µm.

3.6 Tables

Table 3.1 Statistics and supporting data from the linear mixed models for the stand and ramet measurements. Standard error included with diploid and triploid mean. Statistically significant values are in bold.

	Measurement	Diploid	Triploid	Triploid/ Diploid Ratio	n	p-value
Clone Measurements	Basal Area per ground area (m^2/ha)	**17.53 ± 1.80**	**11.37 ± 2.54**	**0.65**	**52**	**0.04**
	Canopy Coverage (% open canopy)	28 ± 5	27 ± 8	0.97	52	0.91
Ramet Measurements	DBH (cm)	10.8 ± 1.4	11.04 ± 2.0	1.03	51	0.89
	Tree Height (meters)	4.7 ± 0.6	5.3 ± 0.9	1.13	51	0.49
	Leaf Area Index (LAI, leaf area per unit ground)	0.78 ± 0.07	0.67 ± 0.10	0.86	42	0.33
	Leaf Area Distal to Branch Segment (cm^2)	432 ± 40	399± 50	0.93	40	0.55
	Hydraulic Conductivity, Kh (kg m^2 s^{-1} MPa^{-1})	$3.58x10^{-8}$± $6.0 x10^{-9}$	$4.68x10^{-8}$± $8.5x10^{-9}$	1.31	40	0.23
	Specific Conductivity , Ks (kg m^{-1} s^{-1} MPa^{-1})	$2.11x10^{-3}$ ± $7.4 x10^{-4}$	$3.37x10^{-3}$± $1.0x10^{-3}$	1.60	40	0.26
	Hydraulic Conductivity normalized by leaf area, Kl (kg m^{-1} s^{-1} MPa^{-1})	$1.16x10^{-6}$ ± $3.1x10^{-7}$	$1.29x10^{-6}$ ± $4.3x10^{-7}$	1.16	40	0.68

Table 3.2 Statistics and supporting data from the linear mixed models for leaf physiology and function. Statistically significant values are in bold.

Measurement	Diploid	Triploid	Triploid/Diploid Ratio	n	F-statistic	p-value
Area per leaf (cm^2)	**13.40 ± 1.52**	**21.10 ± 2.33**	**1.57**	**52**	**$F_{1,8}$ = 10.82**	**0.01**
Dry Mass per leaf (grams)	**0.14 ± 0.01**	**0.24 ± 0.02**	**1.76**	**52**	**$F_{1,8}$ = 24.66**	**<0.01**
Leaf Mass per Area (LMA, mg/cm^2)	**10.2 ± 0.3**	**11.5 ± 0.4**	**1.12**	**52**	**$F_{1,8}$ = 8.17**	**0.021**
Chlorophyll content (SPAD, a unitless index)	**41.42 ± 2.78**	**53.18 ± 3.93**	**1.28**	**51**	**$F_{1,8}$ = 8.96**	**<0.02**
Stomatal length (μm)	**24.70 ± 0.62**	**33.34 ± 0.87**	**1.35**	**52**	**$F_{1,8}$ = 98.86**	**<0.01**
Stomatal density (count per mm^2)	58.47± 4.69	53.76 ± 6.61	0.92	52	$F_{1,8}$ = 0.51	0.50
Stomatal conductance, g_s, (mmol m^{-2} sec^{-1})	**400 ± 19**	**454 ± 26**	**1.14**	**261**	**$F_{1,8}$ = 4.29**	**0.07**
Stomatal conductance, g_s, (mmol m^{-2} sec^{-1}) with log(D) as fixed effect	**Depends on D**			**261**	**$F_{1,193}$ = 7.35**	**<0.01**

Table 3.3 Statistics from the linear mixed models for measurements and surrogates of net assimilation (A). Statistically significant values are in bold.

	Measurement	Diploid	Triploid	Triploid/ Diploid Ratio	n	F-statistic	p-value
A/Ci	V_{cmax}	68.70 ± 3.44	69.47 ± 4.86	1.01	22	$F_{1,8} = 0.03$	0.88
	J_{max}	**129.04 ± 6.10**	**144.98 ± 8.62**	**1.12**	**22**	**$F_{1,8} = 3.42$**	**0.10**
	R_d	2.65 ± 0.52	2.14 ± 0.73	0.81	22	$F_{1,8} = 0.47$	0.51
	Γ*	51.21 ± 1.36	48.23 ± 1.93	0.94	22	$F_{1,8} = 2.39$	0.16
	K_m	970.63 ± 43.58	872.86 ± 61.64	0.90	22	$F_{1,8} = 2.52$	0.15
Fluorometry	Φ_{PSII} (Dark adapted)	0.88 ± 0.003	0.89 ± 0.004	1.01	1142	$F_{1,46} = 1.05$	0.31
	Φ_{PSII} (Light adapted)	**Depends on PAR**			**1017**	**$F_{1,902} = 43.57$**	**<0.01**
	J (light adapted)	Depends on PAR			1017	$F_{1,902} = 2.08$	0.15
	July 2015 α (from curves fit individually)	0.31 ± 0.01	0.29 ± 0.01	0.95	110	$F_{1,8} = 1.29$	0.29
	July 2015 ETR_{max} (from curves fit individually)	302.18 ± 18.19	319.41 ± 25.69	1.06	110	$F_{1,8} = 0.45$	0.52
	June 2016, α (from curves fit individually)	0.31 ± 0.02	0.34 ± 0.02	1.10	18	$F_{1,2} = 1.82$	0.31
	June 2016, ETR_{max} (from curves fit individually)	**113.87 ± 8.35**	**161.06 ± 11.80**	**1.41**	**18**	**$F_{1,2} = 15.98$**	**<0.06**

Table 3.4 Statistics from the linear mixed models for measurements and calculated values related to iWUE and A. Statistically significant values are in bold.

Measurement	Diploid	Triploid	Triploid/Diploid Ratio	n	F-statistic	p-value
$\delta^{13}C$	**-27.46 ± 0.19**	**-26.51 ± 0.27**	**0.97**	**63**	**$F_{1,8}$ = 12.87**	**<0.01**
C_i	**258.35 ± 3.33**	**241.59 ± 4.67**	**0.94**	**63**	**$F_{1,8}$ = 12.87**	**<0.01**
C_i/C_a	**0.65 ± 0.01**	**0.61 ± 0.01**	**0.94**	**63**	**$F_{1,8}$ = 12.87**	**<0.01**
iWUE	**86.88 ± 2.08**	**97.36 ± 2.91**	**1.12**	**63**	**$F_{1,8}$ = 12.87**	**<0.01**
Leaf N % mass	**2.24 ± 0.06**	**2.42 ± 0.08**	**1.08**	**63**	**$F_{1,8}$ = 4.99**	**<0.06**
Leaf C% mass	47.70 ± 0.51	46.93 0.71	0.98	63	$F_{1,8}$ = 1.17	0.31
C:N	**21.42 ± 0.60**	**19.54 ± 0.84**	**0.91**	**63**	**$F_{1,8}$ = 4.99**	**<0.06**

Table 3.5 Calculations for leaf nitrogen in aspen

Measurement	Diploid	Triploid	Triploid/Diploid Ratio
Average mass of leaf nitrogen per leaf area (mmol m^{-2})	162.78	198.48	1.20
Total average mass of nitrogen per leaf (mmol)	0.22	0.42	1.91
Mass of leaf nitrogen per ground area (mmol m^{-2})	127.08	133.51	1.05

4. Triploid aspen have greater basal area growth and intrinsic water-use efficiency than diploid aspen, but are also at greater risk to drought and higher atmospheric water demand

4.1 Abstract

Quaking aspen with differing cytotypes (i.e., diploids and triploids) express key structural and functional traits differently, and this potentially drives differences in ploidy-climate interactions. Triploid aspen typically grow faster than diploids, and have higher photosynthetic rates, stomatal conductance, and intrinsic water-use efficiency (*iWUE*, the ratio of net carbon assimilation (*A*) to stomatal conductance (g_s) inferred from leaf carbon isotope measurements). However, we do not know how *iWUE* changes over time and relative to climate for the ploidy types. Understanding how *iWUE* varies with climate and ploidy is important as this trait influences susceptibility of aspen clones to Sudden Aspen Decline, which is expected to get worse with climate warming. In this study, we used dendrochronology techniques and measurements of carbon isotopes to quantify differences in basal area increment (BAI) and *iWUE* between aspen ploidy types to assess potential differences in ploidy-climate interactions. We found that diploid BAI and *iWUE* were each lower than in triploid aspen. We also found that BAI in diploid aspen correlated positively with the last day of snow and yearly total precipitation, and that BAI in triploid aspen correlated with yearly total precipitation and yearly average vapor pressure deficit (VPD). Furthermore, while both cytotypes increased *iWUE* when precipitation was low and atmospheric water demand was high, triploids maintained almost 4% greater *iWUE* and greater *A* and g_s across all years. However, because triploid

aspen reduce A and g_s less relative to low precipitation and high VPD, we conclude that triploid aspen are actually more prone to drought stress.

4.2 Introduction

In the years 2002 and 2003, heat and drought stress led to widespread mortality in quaking aspen (*Populus tremuloides* Michx.), deemed Sudden Aspen Decline (SAD). SAD is typified by rapid root and branch hydraulic failure that either results in rapid whole-tree death (from roots to crown), or instead drives secondary effects, like fungal infections, that eventually lead to mortality. SAD events are expected in the future as the climate continues to warm (L. D. Anderegg et al., 2013; Anderegg et al., 2014; Anderegg et al., 2012; W. R. Anderegg et al., 2013; Huang & Anderegg, 2012; Worrall et al., 2013). Polyploidy, which is common in southern aspen sub-populations, may affect the climate sensitivity of certain populations because diploid and triploid aspen may have differences in the expression of their structural and functional traits that drive interactions with climate (Mock et al., 2012). In Chapter 3, we found that diploid aspen clones growing in a stand in Colorado had smaller leaves with less chlorophyll, lower nitrogen content, lower maximum photosynthetic rates and lower stomatal conductance than triploid clones. Furthermore, triploid clones had higher leaf-scale intrinsic water-use efficiency, *iWUE*, which is the ratio of net carbon assimilation (A) to stomatal conductance (g_s) inferred from leaf carbon isotope measurements. Nevertheless, despite greater *iWUE*, stomata of triploid aspen were also less responsive to vapor pressure deficit leading to greater maximum transpiration rates, implying that triploid aspen might be more susceptible to drought stress. A separate study in Utah found that, overall,

diploid aspen trees grew more slowly than triploid trees, and that both ploidy types increased basal are increment (BAI) more in cool wet years, and less during warm and dry years (DeRose et al., 2014). However, beyond overall changes in BAI in response to climate, it is unknown how other factors important to drought resistance, like *iWUE*, might different between ploidy types relative to climate over time.

Water-use efficiency is important factor in drought resistance and heat tolerance in plants because greater water-use efficiency can increase plant fitness, though not always (Nicotra & Davidson, 2010). One of the metrics of water-use efficiency, *iWUE*, can be increased by increasing carbon uptake relative to plant water loss, or by reducing plant water loss relative to carbon uptake. At the plant scale, a myriad of plant structural changes and life history strategies can increase carbon uptake, including increasing chlorophyll or nitrogen content per unit leaf area. Alternatively, water loss through transpiration can be reduced by lowering overall stomatal conductance or by increasing plant sensitivity to changes in atmospheric water demand by reducing stomatal conductance relative to increases in vapor pressure deficit (VPD) (Bonan, 2002; Brooks & Coulombe, 2009; Brooks & Mitchell, 2011; Clearwater & Meinzer, 2001; Nicotra & Davidson, 2010; Oren et al., 1999). However, changes to either photosynthetic rate or to stomatal conductance can also result in a concomitant change in the other (Bonan, 2002). Furthermore, the importance of *iWUE* to plant fitness is variable, and a high *iWUE* is not always correlated with plant fitness in drought-prone environments (Condon et al., 2004). For example, some species living in places with dry seasons or high variability in available water may actually have lower *iWUE* because these plants have phenologies

that avoid dry periods and that need to maximize carbon assimilation during short windows of time (Arntz & Delph, 2001; Lisa A. Donovan et al., 2007; Lisa A Donovan & Ehleringer, 1994; Geber & Dawson, 1997; Nicotra & Davidson, 2010; Pennington et al., 1999).

In aspen, the differences in maximum photosynthetic rate, stomatal conductance and stomatal responsiveness to VPD and *iWUE* between diploid and triploid clones exemplify intraspecific differences in life history strategies. These differences potentially explain a suite of interesting observations about aspen. For example, triploid aspen are almost entirely confined to the warmest and driest habitats this species occupies. In addition, the larger aspen clones tend to be triploid and the regions where triploids are most frequent are also known for having aspen's largest stands (Callahan et al., 2013; Greer et al., 2016; Jelinski & Cheliak, 1992; Mitton & Grant, 1996; Mock et al., 2012; Mock et al., 2008). Perhaps these patterns are explained in part because triploid aspen have greater carbon assimilation rates that support faster growth than diploids, and greater triploid *iWUE* allows longer persistence than diploids in the landscape, although this has not been studied (Mock et al., 2008). Furthermore, while there has been widespread die off in quaking aspen, at finer scales, co-occurring clones can have large differences in stem mortality that could be related to ploidy. However, the ploidy types of SAD-affected clones are as of yet unknown. Thus, understanding *iWUE* differences between ploidy types over time and relative to climate drivers would help scientists better understand these phenomena.

In this study, we further explore the structural and functional consequences of polyploidy in aspen. Using dendrochronology techniques, we quantified how diploid and triploid aspen clones differ in BAI and *iWUE* over recent decades, with a focus on very dry and wet years. In addition, by assessing BAI and *iWUE* relationships, our goal was to understand whether ploidy types differ in their susceptibility to climate-driven mortality. To this end, we collected tree cores from co-occurring diploid and triploid clones from a stand in Colorado, measured basal area increments and *iWUE*, and compared these measurements to climate over time.

4.3 Methods

4.3.1 Site

We measured the same aspen clones measured in Chapter 3, found on the western slope of the continental divide in the Rocky Mountains of Colorado (at 2750 meters above sea level) near Almont, Colorado (38.716N, 106.819W). The aspen were on top of a small hill, in close proximity, and in similar soils and slope positions. The average of summer and winter temperature and precipitation measured at three nearby weather stations (Crested Butte, Gunnison, and Taylor Park) are as follows: average summer temperature (May – September) was 11.3 °C and the average winter (October – April) temperature was -5.2 °C. The average total summer precipitation was 19.1 cm and average total winter precipitation was 21.6 cm (Global Historical Climate Network Dataset (GHCN), http://www.ncdc.noaa.gov/cdo-web/).

The aspen stand had a mix of co-occurring diploid and triploid clones and we measured growth (as BAI calculated from ring widths) and intrinsic water-use efficiency (inferred

from the carbon isotope composition of tree-ring cellulose) in 10 spatially segregated clones, of which five were diploid and five were triploid (Figure 3.1).

Within each clone, we selected and cored four ramets of similar size, for a total of 20 ramets for each ploidy type. The diameter of each ramet at 1.3 meters above ground was similar between ploidy types (mean DBH was 10.8 cm and 11.0 cm, respectively).

4.3.2 Chronologies

We extracted three 4.3-mm-wide cores that punched through the entire width of the ramet through its center from one cardinal direction (perpendicular to the direction of slope in the immediate vicinity). The cores were within 1 cm of each other vertically in the ramet. All of the tree cores were mounted with Elmer's glue to grooved boards (with the xylem vessels oriented vertically), and sanded with increasingly finer sandpaper and polishing paper until the ring-width boundaries were clearly visible through a microscope with 200X zoom.

The tree-ring series were crossdated using 2002 and 2012 as marker years, as they were consistently very narrow across cores. Ring widths for each year were subsequently measured and dated to 0.1 mm accuracy using a Velmex measuring station (Velmex Inc.). During crossdating, some cores had missing rings because the ring boundaries were unclear, or because of heart rot. Therefore, for continued study, we selected two cores from three ramets in each clone (6 cores per clone, measured from the same side of the tree) with the longest complete chronologies. We then used the computer program COFECHA (Grissino-Mayer, 2001) to verify crossdating of these 60 diploid and triploid cores, finding the average correlation with the master chronology to be > 0.536. We

calculated basal area increment (BAI) using yearly ring widths and the distance to the pith using the 'dplR' R package (R version 3.3.1 and package version 1.6.4 (Bunn, 2008, 2010)). If the core missed the pith, we estimated the pith distance to the innermost ring by triangulating its likely location by drawing three lines perpendicular to the tangent of the circle of the innermost ring, and measuring the distance from the pith to the innermost ring using the shortest line (see Figure 2 in Hietz (2011)). To account for tree age-related effects, we then detrended BAI for each ploidy type using a negative exponential curve (also using 'dplR').

4.3.3 iWUE

To measure diploid and triploid *iWUE* in our tree cores, we used two sample groupings. For the first group we selected rings using the mean precipitation of three nearby weather stations (Crested Butte, Gunnison, and Taylor Park). We chose years with the lowest precipitation (2002 and 2012), one year with above-average precipitation (1995), and one year with average precipitation (2009) in three ramets in each of the 10 clones (4 years x 3 ramets x 10 clones = 120 samples, see section 4.3.4). For the second grouping, we used complete tree ring series from 1980 to 2014 from two ramets in two diploid and triploid clones (35 years x 2 ramets x 4 clones = 280 samples). For all samples, we measured $\delta^{13}C$ and calculated *iWUE* (equations 1 & 2) as described below.

For each ring, we cut each ring from the core using a razor blade, ground each ring to a fine powder by agitating them in steel vials with steel balls, extracted holo-cellulose from the ground material (Leavitt & Danzer, 1993) and measured $\delta^{13}C$ using continuous-flow isotope ratio mass spectrometry at Oregon State University's Stable Isotope lab in

Corvallis, Oregon. Samples were combusted in a Carlo Erba elemental analyzer and isotope-ratios and percent mass were measured using a Thermo DeltaPlus isotope ratio mass spectrometer. The standard deviation of 45 sample replicates for $\delta^{13}C$ was 0.19 ‰. We derived *iWUE* using equations 1 and 2 (as described in Seibt et al. (2008)):

$$iWUE = \frac{A}{g_s} = \frac{(C_a - C_i)}{1.6}, \qquad (1)$$

where A is the net carbon assimilation, and g_s is stomatal conductance to water vapor. Intercellular [CO_2] (C_i) was estimated from measurements of cellulose $\delta^{13}C$, and measurements of the summer (May – September) mean yearly carbon isotope ratio of atmospheric CO_2 ($\delta^{13}C_a$) and atmospheric [CO_2] (C_a) measured at Niwot Ridge, Colorado (White & Vaughn, 2011) following the model of G.D. Farquhar et al. (1982):

$$\delta^{13}C \approx \delta^{13}C_a - a - (b - a)(\frac{C_i}{C_a}), \qquad (2)$$

where, a is the fractionation against $^{13}CO_2$ during molecular diffusion through the stomata (4.4‰), and b is net fractionation due to carboxylation by the Rubisco enzyme (~27‰). The above model does not include other fractionation factors, and we likely over-estimate C_i (Cernusak & Kahmen, 2013; Leavitt & Danzer, 1993). However, the magnitude of our overestimate is likely small and equal by ploidy type.

For the first group of tree rings (from 1995, 2002, 2009 and 2012), we used linear mixed models to compare diploid and triploid *iWUE* where the response variable was BAI, and fixed effects were ploidy type plus year (without interaction), and the random effect was clone identity. For the second group of *iWUE* data (i.e., the complete time series from 1980-2014), we created separate diploid and triploid *iWUE* chronologies, removed lag-1

series autocorrelations using linear regression, and then detrended the data using the 'dplR' package in R.

4.3.4 Climate data

For this study, we were interested in whether BAI and *iWUE* were similar between ploidy types, and how BAI and *iWUE* varied relative to climate (Figure 4.1). Previous work in aspen has highlighted the importance of temperature, precipitation, vapor pressure deficit (VPD) and potential evapotranspiration (PET) in the distribution of this species and for SAD mortality (Greer et al., 2016; Hogg & Hurdle, 1997; Mock et al., 2012; Worrall et al., 2013). In this study, we compared each year's BAI and *iWUE* to each year's monthly mean temperature maximum, minimum, and mean, and total precipitation, using the monthly means or total of each variable measured at three nearby weather stations (Crested Butte, Gunnison, and Taylor Park, Colorado (Menne et al., 2012)). Also, we compared BAI and *iWUE* to each years' monthly VPD, which we calculated from monthly temperature maximum and temperature minimums using the following formula modified from Bartos and Campbell (1998): $VPD = 0.62 * (esat_{max} - esat_{min})$ where $esat_{max} = 6.112 * e^{\left(17.67 * \frac{\text{tmax}}{\text{tmax} + 243.5}\right)}$ and $esat_{min} = 6.112 * e^{\left(17.67 * \frac{\text{tmin}}{\text{tmin} + 243.5}\right)}$, where tmax is the monthly mean temperature maximum and tmin is the monthly mean temperature minimum. We also compared BAI and *iWUE* to each years' monthly Hargreaves climate moisture deficit (CMD) which was available from ClimateWNA (http://www.climatewna.com/, downloaded October 2016). CMD is a complex climate variable that describes the amount of water needed to offset atmospheric water demand and is calculated as the sum of the monthly difference between reference atmospheric

evaporative demand (E_{ref}) and precipitation. E_{ref} was modeled using methodology from Hargreaves (Hargreaves & Samani, 1982; Shuttleworth, 1993; Wang et al., 2012). We also compared BAI and *iWUE* to each year's first day of the season with zero snow on the ground as measured by Billy Barr at the Rocky Mountain Biological Laboratory (DOY.s).

For the years in the first *iWUE* grouping (1995, 2002, 2009, and 2012), we found that the years 2002 and 2012 had lower water availability, and that the years 1995 and 2009 had greater water availability. In 2002 and 2012, precipitation was 28% lower (1.89 standard deviations from the mean), and 26% lower than the mean (1.78 standard deviations from the mean), respectively. VPD in 2002 and 2012 was also 8% greater (1.3 standard deviations from the mean) and 17% greater than the mean (3.0 standard deviations from the mean), respectively. Precipitation in 1995 and 2009 was 28% greater and 3% less than the mean, respectively (being 1.92 and 0.17 standard deviations from the mean). VPD in 1995 and 2009 was 6% and 6% lower, respectively, than the mean (1.1 and 1.05 standard deviations from the mean).

4.3.5 Statistics

To quantify diploid and triploid differences in BAI or *iWUE* relative to climate, we first fit random forest models for each ploidy type using the randomForest R package version 4.6-12 (Liaw & Wiener, 2002) to yearly and quarterly means of each climate variable. These climate means were aggregated as follows: yearly (Y) consisted of the yearly mean for January through December. For the quarterly data, for each year, quarter 1 (Q1) was

the mean for January through March, quarter 2 (Q2) was the mean for April through June, quarter 3 (Q3) was the mean for July through September, and quarter 4 (Q4) was the mean climate for October through December. For precipitation, instead of the means, sums were calculated for each year and quarter. In Random Forest models, the most important variables for predicting BAI or *iWUE* were the variables with the highest percent change in mean squared error (% increase MSE) when removed from the model. To stabilize variable importance, models were permuted 5000 times. Differences in these variables between models indicate different climatic drivers of each model. Afterwards, using the treeclim R package version 2.0.0 (Zang & Biondi, 2015), we tested for significant correlations between BAI or *iWUE* and monthly climate variables that were chosen from the most important variables found in the random forest analysis. Pearson's correlation coefficients between BAI or *iWUE* and the various climate variables were calculated, and then tested for significance using bootstrapping.

4.4 Results

4.4.1 Basal Area Increment

BAI in diploid trees was smaller than triploid trees for every year from 1980 to 2014 (Figure 4.2, Figure 4.3, $p < 0.04$); over time, both diploid and triploid BAI increased slightly (diploid slope = 0.84 mm^2/yr and triploid slope = 3.0 mm^2/yr). Compared to the diploid and triploid mean BAI (221.9 mm^2 and 350.2 mm^2, respectively), 2002 and 2012 had much lower growth (diploid: 105.6 mm^2 and 91.4 mm^2; triploid: 206.2 mm^2 and 122.6 mm^2, respectively). Diploid and triploid growth in the year 2002 were 105.6 mm^2 and 206.1 mm^2, respectively, and in the year 2012, 91.4 mm^2 and 122.6 mm^2,

respectively. The year with the largest BAI was 2014 (diploid: 366.6 mm^2, triploid: 654.0 mm^2). The random forest models for BAI and climate variables for diploid and triploids explained 25.08% and 25.72% of the total variance. For diploids, the most important variables were DOY.s, yearly mean VPD, yearly total precipitation, and Q1 total precipitation. For triploids, the most important variable were Q3 CMD, yearly mean temperature maximum, yearly mean VPD, and yearly total precipitation (Figure 4.4). We tested for significant Pearson's correlations between BAI and each of these variables: we found that BAI of diploid trees was significantly correlated with DOY.s and yearly total precipitation ($r = 0.266$ for each), and that BAI of triploid trees was correlated with yearly total precipitation and yearly average VPD ($r = 0.298$, and $r = -0.211$, respectively).

4.4.2 iWUE

Calculations of *iWUE* for the subset of measurements (1995, 2002, 2009, and 2012 years only) showed that *iWUE* was significantly higher in triploid trees than in diploid trees for each year: *iWUE* was higher in warmer and drier years than cooler and wetter years for both ploidy types (Table 4.1, Figure 4.5, $n = 120$ for 4 years or 30 per year, $p < 0.005$). Higher BAI also corresponded to lower *iWUE*, and lower BAI corresponded to higher *iWUE*. Calculations of *iWUE* from the eight complete series for 1980 to 2014 (second grouping) show that *iWUE* varied strongly from year to year, and was lower during wetter and cooler years (Figure 4.6). Across all years in this grouping, triploid aspen had greater *iWUE* than diploids ($n = 272$ for 34 years or 8 per year, $p< 0.003$ for a paired t-test using year for pairing). Random forest models for diploids and triploids for *iWUE*

showed that important climate variables varied by ploidy type and were inconclusive for triploids: the percent of variance explained by diploids was 15.96%, with Q1 temperature maximum, Q1 VPD, and Q1 temperature mean being the most important variables (Figure 4.7). In diploids, Q1 temperature maximum and Q1 VPD also had statistically significant Pearson's correlation coefficients (r = 0.26 for both variables). In triploids, percent of variance explained by the random forest model was only 2.98% and successive models had extreme variations in variable importance (results not shown). We also did not find statistically significant Pearson's correlations between triploid *iWUE* and any climate variable. Therefore, we conclude that our model does not show that triploid *iWUE* and climate correlate.

4.5 Discussion

Diploid aspen were found to have lower average BAI and *iWUE* than triploid aspen, and BAI and *iWUE* correlated with climate variables related to water availability. We found that triploid trees had greater overall BAI than diploids, with triploid BAI being 58% greater than diploids between 1980 and 2014. This is similar to findings in DeRose et al. (2014) where triploids were also found to grow faster than diploids. During 2014, the year of greatest BAI for both cytotypes, triploid BAI was 78% greater than diploid BAI. In 1995 and 2009 BAI was greater than the mean, with diploid BAI being 24% and 26% greater than the mean, and triploid BAI being 12% and 14% greater than the mean, respectively. Climatically, BAI was correlated positively with yearly total precipitation and DOY.s in diploids and was positively correlated with yearly total precipitation, and negatively correlated with VPD in triploids. Therefore, we conclude that water

availability is the most important control to aspen in our study site. This is noteworthy, because SAD mortality was greatest in landscape positions with lower or more variable water supplies like slope-shoulders (Worrall et al., 2008; Worrall et al., 2010; Worrall et al., 2013), and the primary cause of SAD mortality in most individuals was disruption to tree hydraulic conductance (L. D. Anderegg et al., 2013; Anderegg et al., 2014; Anderegg et al., 2012; W. R. Anderegg et al., 2013).

During 2002, the year known to have triggered SAD in the early 2000's in our study area, we found that diploid and triploid growth was 53% and 41% lower than each ploidy type's respective mean growth. Interestingly, in 2012, BAI was 59% and 65% lower than the mean, and VPD was higher in 2012 than in the well-known 2002 dry year. SAD is considered a multi-year process with direct mortality from initial climate conditions, followed by 'multiyear hydraulic deterioration' in trees that survived the first wave of mortality (Anderegg et al., 2014; W. R. Anderegg et al., 2013). Consequently, most recent aspen mortality in the study area has been lumped into 2002-related SAD, but perhaps SAD-related mortality beginning in 2012 was actually a separate and new SAD event distinct from the early 2000's SAD. However, 2012 is not well known as a 'SAD year', and perhaps we did not see widespread mortality in 2012 because the most vulnerable ramets had already died from past SAD and were not replaced in the landscape. It is also possible that by 2012 aspen clones were less vulnerable to drought impacts than in 2002-2003 for a variety of reasons ranging from better plant hydraulic conditions (like better root to shoot ratios) or lower overall transpiration which may have

reduced drought impacts (Forde, 2009; Nicotra & Davidson, 2010). Regardless, disentangling SAD impacts from climate in 2002 and 2012 is challenging. Comparisons between BAI and the first group of *iWUE* data revealed that high BAI corresponded to low *iWUE* (and vice versa): during 2002 and 2012, BAI was low and *iWUE* high, and during 1995 and 2009 BAI was high, and *iWUE* low. During these years, measurements of *iWUE* were also 4.1% (4.7 on average) greater in triploid trees than diploid trees, and greater on average in the complete *iWUE* series for 1980 to 2014. Greater triploid *iWUE* in tree rings corresponds with *iWUE* previously measured in leaves where triploid aspen had 12% greater *iWUE* than diploids. Previously, it was also found that both greater overall *A* and g_s in triploids (see Chapter 3) drove greater triploid leaf *iWUE* and we suspect this was also true for *iWUE* measured in this study. Greater triploid *A* in tree rings is likely because BAI was larger in triploids than diploids across all years (including 1995, 2002, 2009, and 2012). For g_s, we previously learned that while both ploidy types reduced g_s as VPD increased, diploids reduced g_s more than triploids at higher VPD (illustrating greater sensitivity to VPD). Interestingly, however, this did not result in overall lower diploid *iWUE* than triploids in 2002 and 2012, nor changes to the 4.1% percent difference in *iWUE* between ploidy types among years. Instead, triploids maintained a 4.1% greater *iWUE* across all years, which we speculate is because relative increases in triploid *A* offset greater reductions in diploid g_s in 2002 and 2012. This follows other studies in other species where a greater *A* has led to higher *iWUE* (Brooks & Coulombe, 2009; Brooks & Mitchell, 2011; Clearwater & Meinzer, 2001; Lisa A. Donovan et al., 2007; Nicotra & Davidson, 2010). However, the consequence of triploid

aspen maintaining higher *A* and g_s than diploid aspen during high VPD and low water availability is that while carbon gain is maximized, so is risk to hydraulic failure: triploids would need a greater total water supply than diploids to maintain higher water losses during these demanding conditions. We speculate that these differences illustrate different adaptive strategies in aspen with diploids being more conservative and triploids being more risky in their growth and water loss. This could explain why the triploid *iWUE* time series data did not correspond to climatic changes: triploids may not modulate *A* or g_s in response to climate to the same degree as diploids. Furthermore, Pando, and other large aspen clones are triploids and their greater relative size could be fueled by high A over both wet and dry climatic conditions (Kemperman & Barnes, 1976; Mock et al., 2012; Mock et al., 2008). As an alternate hypothesis, it is possible that, overall, triploid trees were actually not as water stressed as diploids which would explain why they were less sensitive to increases to VPD. However, we previously found that triploid aspen stands had 38% fewer ramets per unit ground area; we suspect that triploid aspen clones could require a greater root to shoot ratio to maintain high g_s. Also, we found greater relative BAI reductions in triploids than diploids in the years 2002 and 2012. Therefore, we conclude that at our study site, triploid aspen may be more sensitive to concomitant increases in vapor pressure deficit than diploids, and that the ploidy types could have different susceptibility to SAD. However, it is unknown if SAD in the early 2000s was more common in diploid or triploid clones. While maps of clone boundaries and ploidy identity have been created in a handful of locations, widespread maps of clone boundaries do not exist and most aspen clone ploidy levels are unknown (Mock et al.,

2012; Mock et al., 2008). If these data were measured in more locations across North America, these data would help scientists and land managers better understand and predict SAD impacts. Regardless, our research suggests that aspen ploidy type is an important dynamic to forest mortality in North America.

4.6 Figures

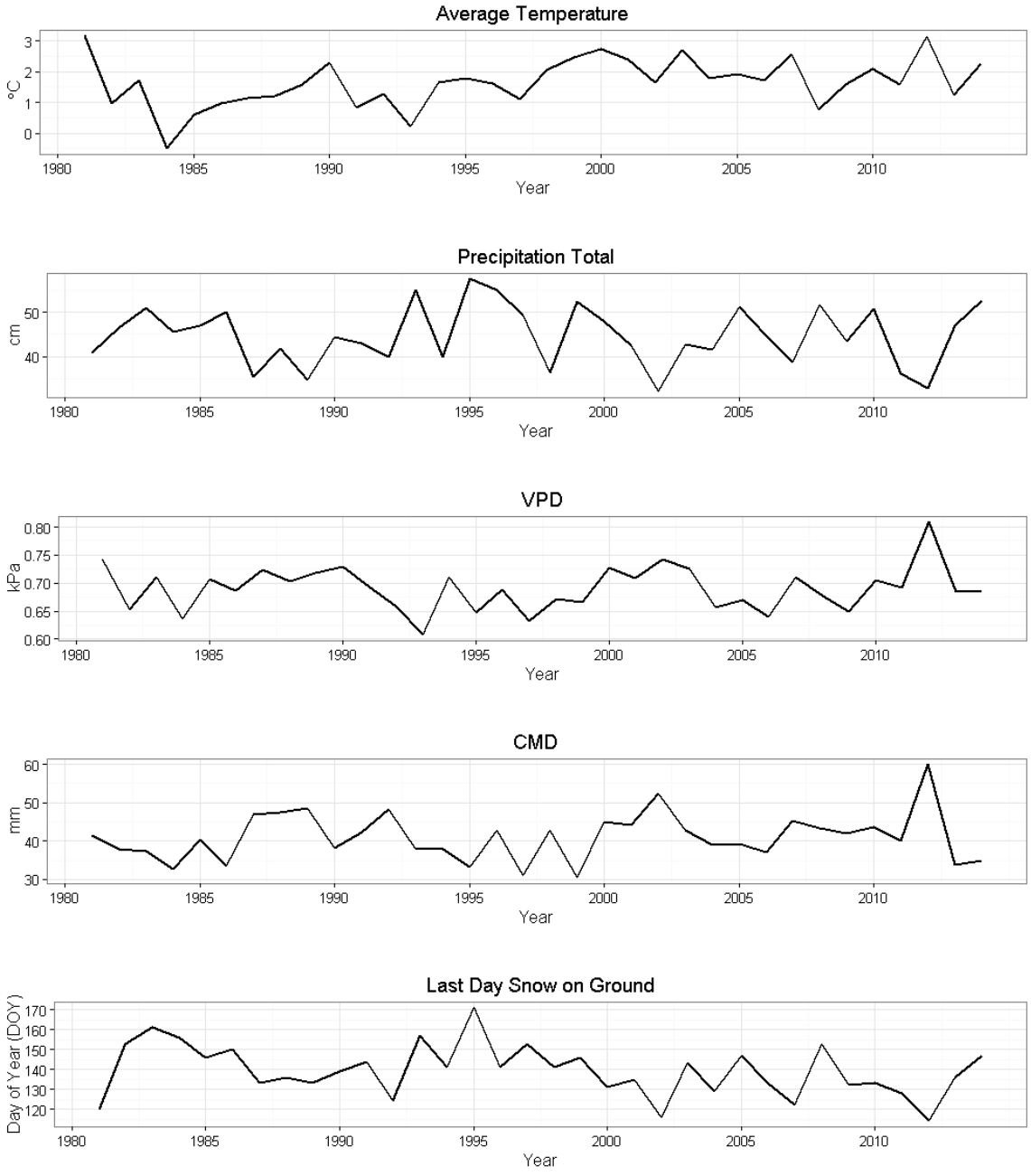

Figure 4.1 Yearly climate from monthly data from 1980 to 2014. All values are yearly means (except for precipitation that is the yearly total). Climate moisture deficit (CMD) describes the amount of water needed to offset atmospheric water demand. Last Day Snow on Ground (DOY.s) is the last day of the season with measureable snow on the ground in the springtime.

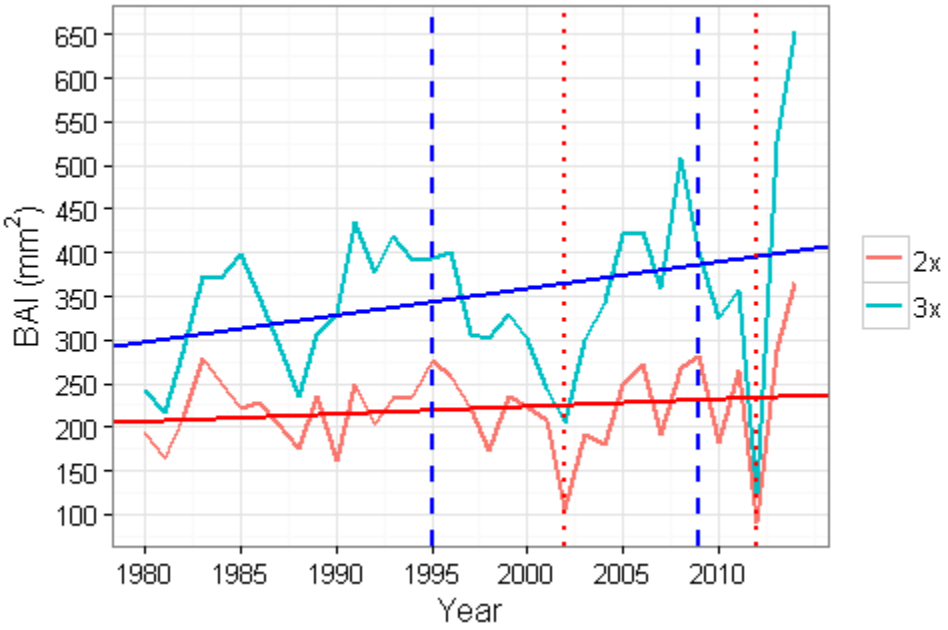

Figure 4.2 Basal Area Increment for diploid and triploid aspen for 1980 to 2014. Lines are the best-fit lines from the linear mixed model. Vertical lines match years used for the first group of iWUE measurements where 1995 and 2009 have higher total precipitation (blue), and 2002 and 2012 have lower total precipitation (red).

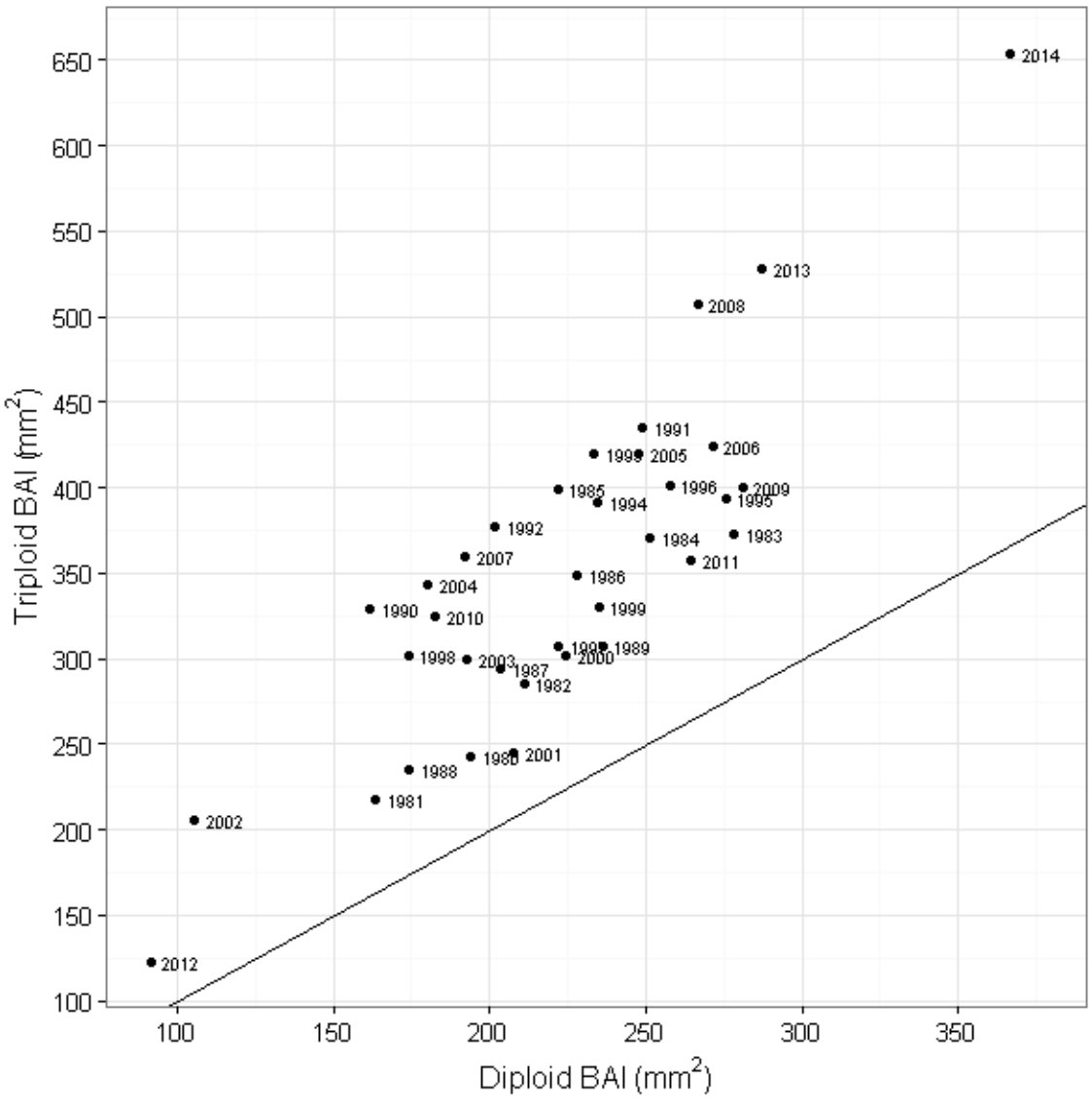

Figure 4.3 Diploid and triploid mean BAI for each year. Line represents where the ratio of diploid to triploid BAI is 1.

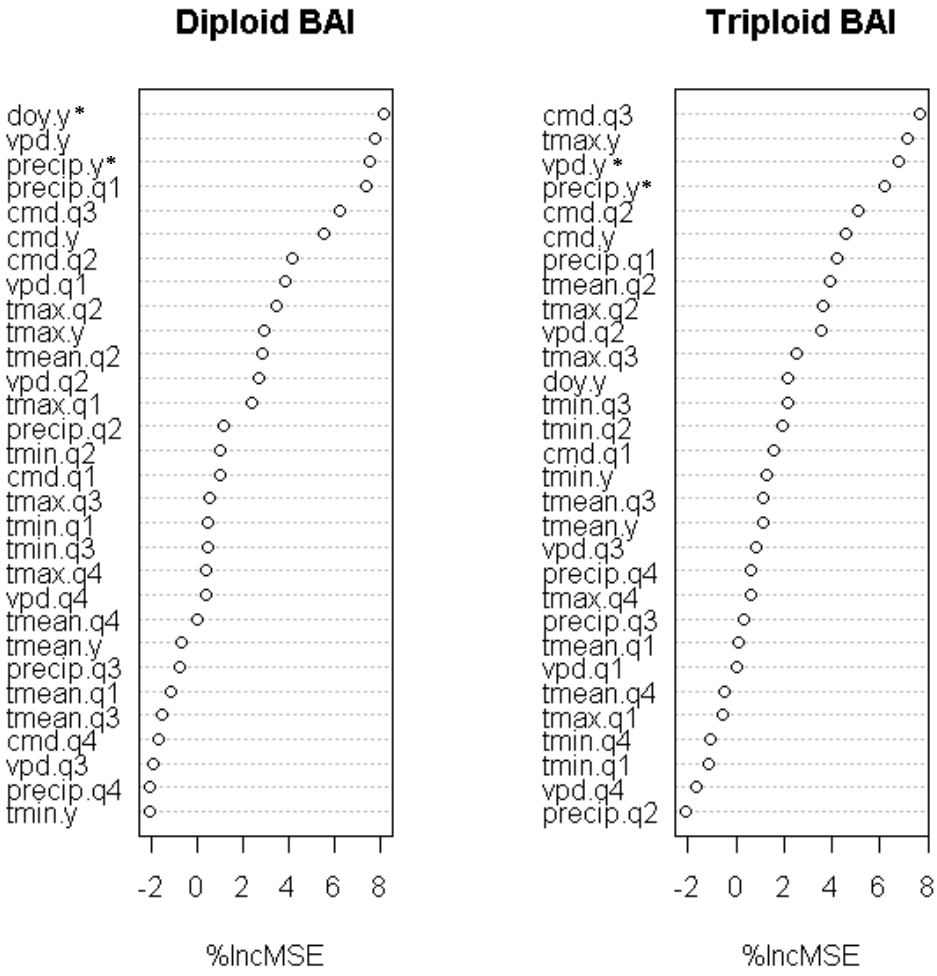

Figure 4.4 Percent change in MSE for diploid and triploid aspen random forest models for each climate variable. Labels with 'y' denotes yearly mean, and 'q1' through 'q4' denote quarterly means. Precipitation measurements are totals (instead of means). Variables with '' had significant correlations with BAI.*

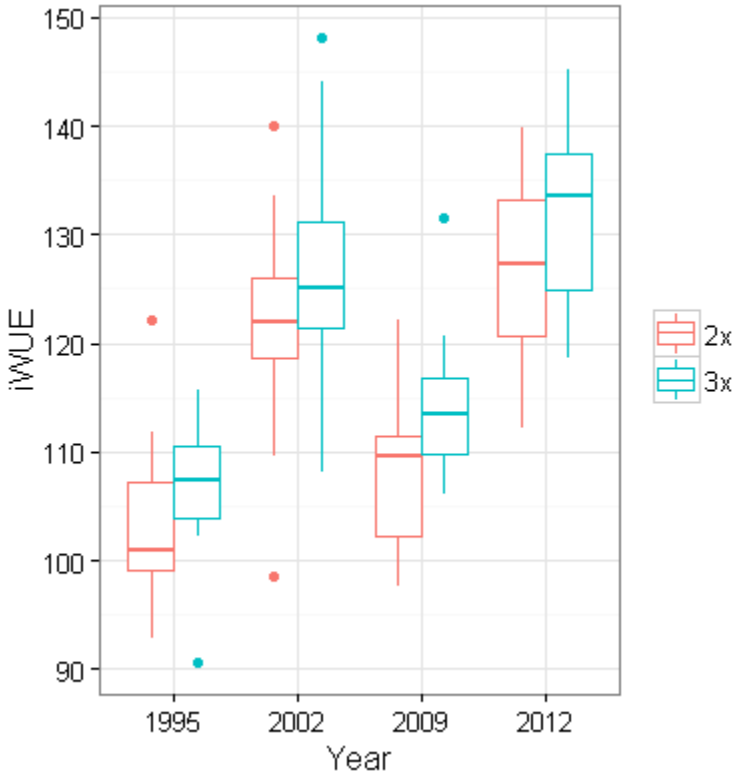

Figure 4.5 Boxplots of iWUE in tree rings for warmer and drier (2002 and 2012) and cooler and wetter (1995, 2009) years. Triploids have higher iWUE than diploids within each year across all years ($p < 0.005$).

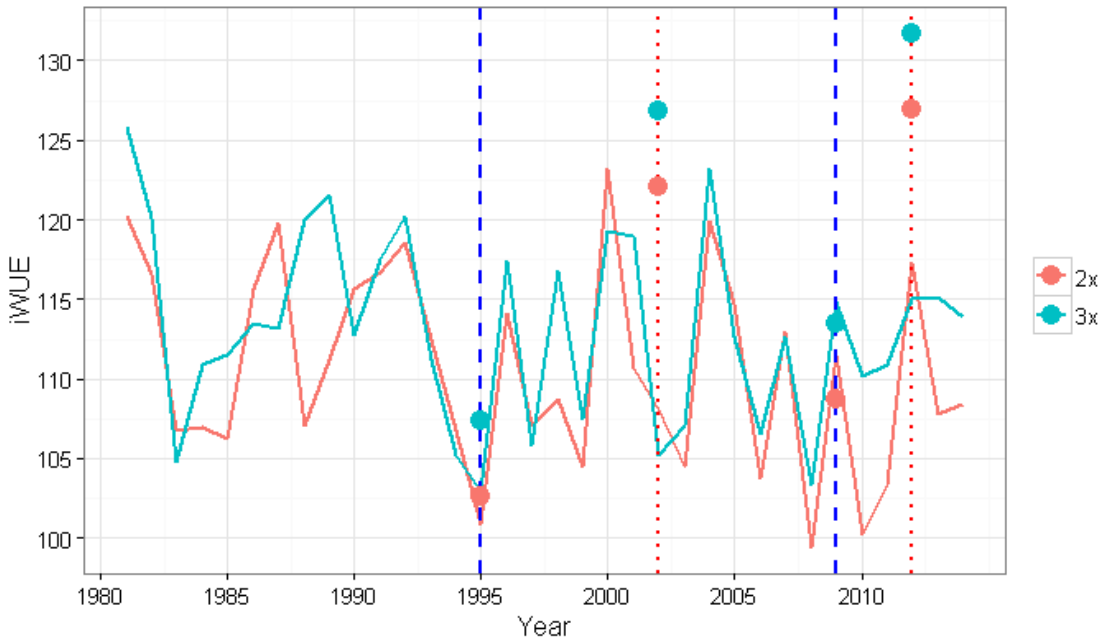

Figure 4.6 iWUE for diploid and triploid aspen. The mean iWUE chronologies are from 2 ramets in 2 clones in each ploidy type (n = 8). The vertical dashed lines represent dry and warm (red), and wet and cool (blue) years. Dots represent Ploidy means from 1995, 2002, 2009, and 2012 for the first group of iWUE data (n = 30 per year).

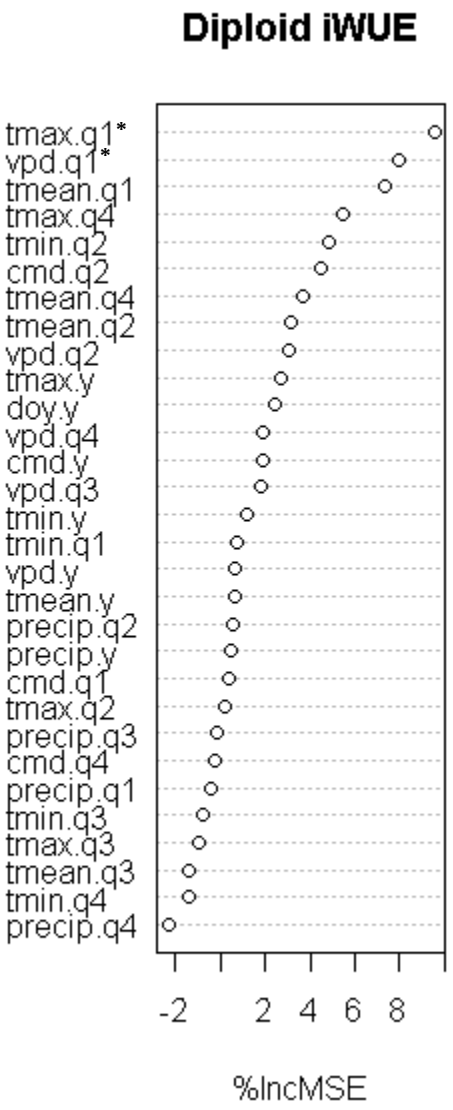

Figure 4.7 Percent change in MSE for diploid aspen random forest models for each climate variable. The triploid Random Forest model explained only 2.98% of the variance and did not correlate with climate data (data not shown). Variables with '' had significant correlations with iWUE.*

Tables

Table 4.1 iWUE (A/g_s) means measured in tree rings from diploid and triploid aspen

	Diploid	Triploid	% Triploid Difference
1995	102.6	107.3	4.5
2002	122.0	126.7	3.8
2009	126.9	131.6	3.7
2012	107.3	112.0	4.3
mean	114.7	119.4	4.1

5. Conclusion

We gained a greater understanding of the mechanisms that drive aspen's biogeography while we explored if genetically similar sub-populations were adapted to the same or different climates, and if there were differences in diploid and triploid structure and function that corresponded to differences in ploidy-climate interactions. First, we discovered that the northern (NC) and southwestern (SC) subpopulations of aspen had different climate niches: the SC distribution was constrained by mean annual precipitation and temperature maximums and the NC distribution was constrained by growing degree days and PET. We also concluded that aspen distribution models should be fit to genetically related subpopulations to more accurately reflect adaptation to local climate. Second, at landscape scales, we discovered that polyploidy was important to aspen-climate interaction because diploid and triploid clones had differences in form and function. We found that diploid aspen had smaller leaves with less chlorophyll, and lower LMA that coincided with lower leaf %N, J_{max}, Φ_{PSII}, and g_s. We also found that triploid aspen reduced g_s less in response to increased VPD (likely because of larger, leakier, stomata), and that *iWUE* was greater in triploid leaves. These findings imply that triploids had greater photosynthetic rates and stomatal conductance than diploids in response to climate and that despite greater *iWUE,* triploids may actually be more prone to climate-induced stress. These interpretations were consistent with ploidy differences in BAI and *iWUE* measured in tree rings: triploid aspen had greater BAI and grew faster than diploids, and had greater *iWUE* in response to climate. We also found that during years with less water availability, both BAI and *iWUE* increased for both diploid and triploids. However, conceptual models illustrated that triploid aspen also reduced A and g_s less than

diploids over time, and that triploids were less sensitive to climate-induced stress. All of these differences suggest alternate life history strategies between ploidy types where triploids have greater potential growth, but are also at greater risk to climate-induced stress because of potentially higher transpiration. While this could have allowed triploids to outcompete diploids in growth during favorable climatic conditions, it also could have resulted in triploid dieback similar to SAD.

This work introduces new questions for future research. First, it remains unclear how our conclusions correspond between macro and local scales. In order to address this question in the future, we can envision a number of approaches. To study if genetic relatedness also drives finer-scale climate adaptation, we could compare climate niche overlap for the smaller genetic clusters found in Callahan et al. (2013). As a separate work, comparisons of niche overlap for diploids and triploids (using ploidy-specific SDMs) would place our findings from Almont in broader context. Also, to upscale our site-specific ploidy data from Almont, Colorado, we could expand our scope of inference and measure aspen structure and function at the study sites in Mock et al. (2012). These places are good starting points because of known ploidy-climate interactions at these sites. In addition, reciprocal transplants and common gardens using trees from these locations could help tease apart genetic (including ploidy) and climatic controls to phenotype and function. Previously, Gray et al. (2011), did similar work in Western Canada for naturally occurring aspen and we could utilize their methods over a broader area while also including ploidy as a variable (which was not a part of Gray et al. (2011)). With these

approaches, we should be able to better connect our macro-scale and local-scale scale findings.

One confounding factor to aspen studies is how clonality affects aspen-climate interactions. Our work revealed that over 50% of the total variance in traits was at the ramet scale (Appendix S8). Given that each ramet in a clone is genetically identical, this could mean that ramet microsites are important to phenotype and that for aspen, multiple samples within clones are necessary to tease out genetic versus environmental drivers to phenotype or climate tolerance. Therefore, we suggest that future studies of aspen ecophysiology measure both between and within clone traits.

Finally, our results could have management implications for mitigating against climate-induced stress and mortality in aspen. Past and projected SAD impacts demonstrate that we must understand aspen-ploidy-climate dynamics in order to properly manage aspen forests. Across North America, aspen are mostly unmanaged, but assisted migration is an approach that could mitigate climate-induced stress in natural populations. (Gray et al., 2011; Hewitt et al., 2011; Jason S McLachlan et al., 2007; Vitt et al., 2010). A framework for evaluating the feasibility of assisted migration describes weighing tradeoffs among ‘confidence in ecological understanding’ and perceived risks of either implementing, or not implementing management (J. S. McLachlan et al., 2007). In aspen, potential targets for assisted migration have been identified in Western Canada, but not for a majority of aspen’s range or for different ploidy levels (Gray et al., 2011; Schreiber et al., 2013). Our data provides an initial framework for analysis of genetics-climate interactions, with a focus on ploidy. However, as outlined above, there is a lot of work remaining to

downscale genetic relatedness and climate adaptation, or upscale ploidy-climate interactions from our dataset in Almont. Therefore, significant further work is required in order to pursue assisted migration before it is too late.

6. References

Allen, R. G., Pereira, L. S., Raes, D., & Smith, M. (1998). Crop evapotranspiration-Guidelines for computing crop water requirements-FAO Irrigation and drainage paper 56. *FAO, Rome, 300*(9), D05109.

Allouche, O., Tsoar, A., & Kadmon, R. (2006). Assessing the accuracy of species distribution models: prevalence, kappa and the true skill statistic (TSS). *Journal of Applied Ecology, 43*(6), 1223-1232. doi: 10.1111/j.1365-2664.2006.01214.x

Anderegg, L. D., Anderegg, W. R., Abatzoglou, J., Hausladen, A. M., & Berry, J. A. (2013). Drought characteristics' role in widespread aspen forest mortality across Colorado, USA. *Glob Chang Biol, 19*(5), 1526-1537. doi: 10.1111/gcb.12146

Anderegg, W. R., Anderegg, L. D., Berry, J. A., & Field, C. B. (2014). Loss of whole-tree hydraulic conductance during severe drought and multi-year forest die-off. *Oecologia, 175*(1), 11-23. doi: 10.1007/s00442-013-2875-5

Anderegg, W. R., Berry, J. A., Smith, D. D., Sperry, J. S., Anderegg, L. D., & Field, C. B. (2012). The roles of hydraulic and carbon stress in a widespread climate-induced forest die-off. *Proc Natl Acad Sci U S A, 109*(1), 233-237. doi: 10.1073/pnas.1107891109

Anderegg, W. R., Plavcová, L., Anderegg, L. D., Hacke, U. G., Berry, J. A., & Field, C. B. (2013). Drought's legacy: multiyear hydraulic deterioration underlies widespread aspen forest die-off and portends increased future risk. *Global Change Biology, 19*(4), 1188-1196.

Araujo, M. B., & New, M. (2007). Ensemble forecasting of species distributions. *Trends Ecol Evol, 22*(1), 42-47. doi: 10.1016/j.tree.2006.09.010

Arntz, M. A., & Delph, L. F. (2001). Pattern and process: evidence for the evolution of photosynthetic traits in natural populations. *Oecologia, 127*(4), 455-467.

Barker, M. S., Husband, B. C., & Pires, J. C. (2016). Spreading Wings and flying high: The evolutionary importance of polyploidy after a century of study. *Am J Bot, 103*(7), 1139-1145. doi: 10.3732/ajb.1600272

Barnes, B. V. (1975). Phenotypic Variation of Trembling Aspen in Western North-America. *Forest Science, 21*(3), 319-328.

Barnes, B. V., & Wagner, W. H. (2002). *Michigan Trees*. Ann Arbor, MI: The University of Michigan Press.

Bartos, D. L., & Campbell, R. B. (1998). Decline of quaking aspen in the interior West--examples from Utah. *Rangelands Archives, 20*(1), 17-24.

Bennett, M., & Leitch, I. (2012). *Angiosperm DNA C-values database*.

Blaine Marchant, D., Soltis, D. E., & Soltis, P. S. (2016). Patterns of abiotic niche shifts in allopolyploids relative to their progenitors. *New Phytologist, 212*(3), 708-718. doi: 10.1111/nph.14069

Bonan, G. B. (2002). *Ecological climatology: concepts and applications*: Cambridge University Press.

Bretfeld, M., Franklin, S. B., & Peet, R. K. (2016). A multiple-scale assessment of long-term aspen persistence and elevational range shifts in the Colorado Front Range. *Ecological Monographs, 86*(2), 244-260.

Brooks, J. R., & Coulombe, R. (2009). Physiological responses to fertilization recorded in tree rings: isotopic lessons from a long-term fertilization trial. *Ecol Appl, 19*(4), 1044-1060.

Brooks, J. R., & Mitchell, A. K. (2011). Interpreting tree responses to thinning and fertilization using tree-ring stable isotopes. *New Phytologist, 190*(3), 770-782.

Bunn, A. G. (2008). A dendrochronology program library in R (dplR). *Dendrochronologia, 26*(2), 115-124. doi: http://dx.doi.org/10.1016/j.dendro.2008.01.002

Bunn, A. G. (2010). Statistical and visual crossdating in R using the dplR library. *Dendrochronologia, 28*(4), 251-258. doi: http://dx.doi.org/10.1016/j.dendro.2009.12.001

Burns, R. M., & Barbara, H. (1990). Silvics of North America: 1. conifers; 2. hardwoods.

Callahan, C. M., Rowe, C. A., Ryel, R. J., Shaw, J. D., Madritch, M. D., & Mock, K. E. (2013). Continental-scale assessment of genetic diversity and population structure in quaking aspen (Populus tremuloides). *Journal of Biogeography, 40*(9), 1780-1791. doi: Doi 10.1111/Jbi.12115

Cernusak, L. A., & Kahmen, A. (2013). The multifaceted relationship between leaf water 18O enrichment and transpiration rate. *Plant Cell and Environment, 36*(7), 1239-1241. doi: Doi 10.1111/Pce.12081

Clearwater, M. J., & Meinzer, F. C. (2001). Relationships between hydraulic architecture and leaf photosynthetic capacity in nitrogen-fertilized Eucalyptus grandis trees. *Tree Physiol, 21*(10), 683-690.

Collatz, G. J., Ball, J. T., Grivet, C., & Berry, J. A. (1991). Physiological and environmental regulation of stomatal conductance, photosynthesis and transpiration: a model that includes a laminar boundary layer. *Agricultural and Forest Meteorology, 54*(2), 107-136.

Condon, A. G., Richards, R., Rebetzke, G., & Farquhar, G. (2004). Breeding for high water-use efficiency. *Journal of experimental botany, 55*(407), 2447-2460.

Coop, J. D., Barker, K. J., Knight, A. D., & Pecharich, J. S. (2014). Aspen (Populus tremuloides) stand dynamics and understory plant community changes over 46years near Crested Butte, Colorado, USA. *Forest Ecology and Management, 318*, 1-12. doi: 10.1016/j.foreco.2014.01.019

DeRose, R. J., Mock, K. E., & Long, J. N. (2014). Cytotype differences in radial increment provide novel insight into aspen reproductive ecology and stand dynamics. *Canadian Journal of Forest Research, 45*(1), 1-8. doi: 10.1139/cjfr-2014-0382

Donovan, L. A., Dudley, S. A., Rosenthal, D. M., & Ludwig, F. (2007). Phenotypic selection on leaf water use efficiency and related ecophysiological traits for natural populations of desert sunflowers. *Oecologia, 152*(1), 13-25. doi: 10.1007/s00442-006-0627-5

Donovan, L. A., & Ehleringer, J. R. (1994). Potential for selection on plants for water-use efficiency as estimated by carbon isotope discrimination. *Am J Bot*, 927-935.

Drake, P. L., Froend, R. H., & Franks, P. J. (2013). Smaller, faster stomata: scaling of stomatal size, rate of response, and stomatal conductance. *J Exp Bot, 64*(2), 495-505. doi: 10.1093/jxb/ers347

Dudley, S. A. (1996). Differing Selection on Plant Physiological Traits in Response to Environmental Water Availability: A Test of Adaptive Hypotheses. *Evolution, 50*(1), 92-102. doi: 10.2307/2410783

Dunford, M. P. (1984). Cytotype Distribution of Atriplex-Canescens (Chenopodiaceae) of Southern New-Mexico and Adjacent Texas. *Southwestern Naturalist, 29*(2), 223-228. doi: Doi 10.2307/3671028

Edwards, L. J., Muller, K. E., Wolfinger, R. D., Qaqish, B. F., & Schabenberger, O. (2008). An R2 statistic for fixed effects in the linear mixed model. *Statistics in medicine, 27*(29), 6137-6157.

Ellsworth, D. S., & Reich, P. B. (1993). Canopy Structure and Vertical Patterns of Photosynthesis and Related Leaf Traits in a Deciduous Forest. *Oecologia, 96*(2), 169-178.

Evans, J. R. (1989). Photosynthesis and Nitrogen Relationships in Leaves of C₃ Plants. *Oecologia, 78*(1), 9-19.

Farquhar, G. D., Ehleringer, J. R., & Hubick, K. T. (1989). Carbon Isotope Discrimination and Photosynthesis. *Annual Review of Plant Physiology and Plant Molecular Biology, 40*(1), 503-537. doi: DOI 10.1146/annurev.arplant.40.1.503

Farquhar, G. D., O'Leary, M. H., & Berry, J. A. (1982). On the relationship between carbon isotope discrimination and the intercellular carbon dioxide concentration in leaves. *Functional Plant Biology, 9*(2), 121-137.

Farquhar, G. v., von Caemmerer, S. v., & Berry, J. (1980). A biochemical model of photosynthetic CO2 assimilation in leaves of C3 species. *Planta, 149*(1), 78-90.

Forde, B. G. (2009). Is it good noise? The role of developmental instability in the shaping of a root system. *Journal of experimental botany, 60*(14), 3989-4002.

Franklin, J. (2010). *Mapping species distributions: spatial inference and prediction*: Cambridge University Press.

Franklin, J. (2013). Species distribution models in conservation biogeography: developments and challenges. *Diversity and Distributions, 19*(10), 1217-1223. doi: 10.1111/ddi.12125

Franks, P. J., Drake, P. L., & Beerling, D. J. (2009). Plasticity in maximum stomatal conductance constrained by negative correlation between stomatal size and density: an analysis using Eucalyptus globulus. *Plant Cell Environ, 32*(12), 1737-1748.

Geber, M. A., & Dawson, T. E. (1997). Genetic variation in stomatal and biochemical limitations to photosynthesis in the annual plant, Polygonum arenastrum. *Oecologia, 109*(4), 535-546.

Grant, M. C., & Mitton, J. B. (1979). Elevational Gradients in Adult Sex-Ratios and Sexual-Differentiation in Vegetative Growth-Rates of Populus-Tremuloides Michx. *Evolution, 33*(3), 914-918. doi: Doi 10.2307/2407654

Gray, L. K., Gylander, T., Mbogga, M. S., Chen, P. Y., & Hamann, A. (2011). Assisted migration to address climate change: recommendations for aspen reforestation in western Canada. *Ecol Appl, 21*(5), 1591-1603.

Greer, B. T., Still, C., Howe, G. T., Tague, C., & Roberts, D. A. (2016). Populations of aspen (Populus tremuloides Michx.) with different evolutionary histories differ in their climate occupancy. *Ecol Evol, 6*(9), 3032-3039. doi: 10.1002/ece3.2102

Grissino-Mayer, H. D. (2001). Evaluating Crossdating Accuracy: A Manual and Tutorial for the Computer Program COFECHA. *Tree-Ring Research, 57*(2), 205-221.

Gylander, T., Hamann, A., Brouard, J. S., & Thomas, B. R. (2012). The Potential of Aspen Clonal Forestry in Alberta: Breeding Regions and Estimates of Genetic Gain from Selection. *Plos One, 7*(8). doi: 10.1371/journal.pone.0044303

Hao, G. Y., Lucero, M. E., Sanderson, S. C., Zacharias, E. H., & Holbrook, N. M. (2013). Polyploidy enhances the occupation of heterogeneous environments through hydraulic related trade-offs in Atriplex canescens (Chenopodiaceae). *New Phytol, 197*(3), 970-978. doi: 10.1111/nph.12051

Hargreaves, G. H., & Samani, Z. A. (1982). Estimating potential evapotranspiration. *Journal of the Irrigation and Drainage Division, 108*(3), 225-230.

Harley, P., Thomas, R., Reynolds, J., & Strain, B. (1992). Modelling photosynthesis of cotton grown in elevated CO2. *Plant Cell Environ, 15*(3), 271-282.

Harley, P. C., & Sharkey, T. D. (1991). An improved model of C3 photosynthesis at high CO2: reversed O2 sensitivity explained by lack of glycerate reentry into the chloroplast. *Photosynthesis Research, 27*(3), 169-178.

Hewitt, N., Klenk, N., Smith, A. L., Bazely, D. R., Yan, N., Wood, S., MacLellan, J. I., Lipsig-Mumme, C., & Henriques, I. (2011). Taking stock of the assisted migration debate. *Biological Conservation, 144*(11), 2560-2572. doi: http://dx.doi.org/10.1016/j.biocon.2011.04.031

Hietz, P. (2011). A simple program to measure and analyse tree rings using Excel, R and SigmaScan. *Dendrochronologia (Verona), 29*(4), 245-250. doi: 10.1016/j.dendro.2010.11.002

Hijmans, R. J., Cameron, S. E., Parra, J. L., Jones, P. G., & Jarvis, A. (2005). Very high resolution interpolated climate surfaces for global land areas. *International Journal of Climatology, 25*(15), 1965-1978. doi: Doi 10.1002/Joc.1276

Hijmans, R. J., Gavrilenko, T., Stephenson, S., Bamberg, J., Salas, A., & Spooner, D. M. (2007). Geographical and environmental range expansion through polyploidy in wild potatoes (Solanum section Petota). *Global Ecology and Biogeography, 16*(4), 485-495. doi: DOI 10.1111/j.1466-8238.2007.00308.x

Hogg, E. H., & Hurdle, P. (1997). Sap flow in trembling aspen: implications for stomatal responses to vapor pressure deficit. *Tree Physiol, 17*(8-9), 501-509.

Hsiao, T. C., & Acevedo, E. (1974). Plant responses to water deficits, water-use efficiency, and drought resistance. *Agricultural meteorology, 14*(1-2), 59-84.

Huang, C. Y., & Anderegg, W. R. L. (2012). Large drought-induced aboveground live biomass losses in southern Rocky Mountain aspen forests. *Global Change Biology, 18*(3), 1016-1027. doi: DOI 10.1111/j.1365-2486.2011.02592.x

Hunter, K. L., Betancourt, J. L., Riddle, B. R., Van Devender, T. R., Cole, K. L., & Spaulding, W. G. (2001). Ploidy race distributions since the Last Glacial Maximum in the North American desert shrub, Larrea tridentata. *Global Ecology and Biogeography, 10*(5), 521-533. doi: DOI 10.1046/j.1466-822X.2001.00254.x

Jarvis, P. (1976). The interpretation of the variations in leaf water potential and stomatal conductance found in canopies in the field. *Philosophical Transactions of the Royal Society of London B: Biological Sciences, 273*(927), 593-610.

Jelinski, D. E., & Cheliak, W. M. (1992). Genetic Diversity and Spatial Subdivision of Populus tremuloides (Salicaceae) in a Heterogeneous Landscape. *Am J Bot, 79*(7), 728-736.

Kemperman, J. A., & Barnes, B. V. (1976). Clone size in American aspens. *Canadian Journal of Botany, 54*, 2603-2607.

Kira, T. (1991). Forest Ecosystems of East and Southeast-Asica in a Global Perspective. *Ecological Research, 6*(2), 185-200. doi: 10.1007/bf02347161

Kirkpatrick, M., & Barton, N. H. (1997). Evolution of a Species' Range. *The American Naturalist, 150*(1), 1-23. doi: 10.1086/286054

Lande, R., & Shannon, S. (1996). The role of genetic variation in adaptation and population persistence in a changing environment. *Evolution, 50*(1), 434-437.

Lawson, T., & Blatt, M. R. (2014). Stomatal size, speed, and responsiveness impact on photosynthesis and water use efficiency. *Plant Physiol, 164*(4), 1556-1570.

Leavitt, S. W., & Danzer, S. R. (1993). Method for batch processing small wood samples to holocellulose for stable-carbon isotope analysis. *Analytical Chemistry, 65*(1), 87-89.

Levitt, J. (1980). *Responses of plants to environmental stresses. Volume II. Water, radiation, salt, and other stresses*: Academic Press.

Li, H. T., Wang, X. L., & Hamann, A. (2010). Genetic adaptation of aspen (Populus tremuloides) populations to spring risk environments: a novel remote sensing approach. *Canadian Journal of Forest Research-Revue Canadienne De Recherche Forestiere, 40*(11), 2082-2090. doi: 10.1139/X10-153

Li, W.-L., Berlyn, G. P., & Ashton, P. M. S. (1996). Polyploids and their structural and physiological characteristics relative to water deficit in Betula papyrifera (Betulaceae). *Am J Bot*, 15-20.

Liaw, A., & Wiener, M. (2002). Classification and regression by randomForest. *R news, 2*(3), 18-22.

Ling, Q., Huang, W., & Jarvis, P. (2011). Use of a SPAD-502 meter to measure leaf chlorophyll concentration in Arabidopsis thaliana. *Photosynthesis Research, 107*(2), 209-214. doi: 10.1007/s11120-010-9606-0

Little, J., E.L. (Ed.) (1971) (Vols. Miscellaneous Publication 1146. Digitized 1999 by US Geological Survey.). US Department of Agriculture.

Madlung, A., & Wendel, J. (2013). Genetic and epigenetic aspects of polyploid evolution in plants. *Cytogenetic and genome research, 140*(2-4), 270-285.

Maherali, H., Walden, A. E., & Husband, B. C. (2009). Genome duplication and the evolution of physiological responses to water stress. *New Phytologist, 184*(3), 721-731.

Manzaneda, A. J., Rey, P. J., Bastida, J. M., Weiss-Lehman, C., Raskin, E., & Mitchell-Olds, T. (2012). Environmental aridity is associated with cytotype segregation and polyploidy occurrence in Brachypodium distachyon (Poaceae). *New Phytol, 193*(3), 797-805. doi: 10.1111/j.1469-8137.2011.03988.x

Martin, T. A., Hinckley, T. M., Meinzer, F. C., & Sprugel, D. G. (1999). Boundary layer conductance, leaf temperature and transpiration of Abies amabilis branches. *Tree Physiol, 19*(7), 435-443. doi: 10.1093/treephys/19.7.435

Massonnet, C., Costes, E., Rambal, S., Dreyer, E., & Regnard, J. L. (2007). Stomatal Regulation of Photosynthesis in Apple Leaves: Evidence for Different Water-use Strategies between Two Cultivars. *Ann Bot, 100*(6), 1347-1356. doi: 10.1093/aob/mcm222

Maxwell, K., & Johnson, G. N. (2000). Chlorophyll fluorescence—a practical guide. *Journal of experimental botany, 51*(345), 659-668.

McLachlan, J. S., Hellmann, J. J., & Schwartz, M. W. (2007). A framework for debate of assisted migration in an era of climate change. *Conservation Biology, 21*(2), 297-302.

McLachlan, J. S., Hellmann, J. J., & Schwartz, M. W. (2007). A framework for debate of assisted migration in an era of climate change. *Conserv Biol, 21*(2), 297-302. doi: 10.1111/j.1523-1739.2007.00676.x

Menne, M., Durre, I., Korzeniewski, B., McNeal, S., Thomas, K., Yin, X., Anthony, S., Ray, R., Vose, R., & Gleason, B. (2012). Global historical climatology network-daily (GHCN-Daily), Version 3.22. *NOAA National Climatic Data Center*.

Mitton, J. B., & Grant, M. C. (1996). Genetic variation and the natural history of quaking aspen. *BioScience, 46*(1), 25-31. doi: Doi 10.2307/1312652

Mock, K. E., Callahan, C. M., Islam-Faridi, M. N., Shaw, J. D., Rai, H. S., Sanderson, S. C., Rowe, C. A., Ryel, R. J., Madritch, M. D., Gardner, R. S., & Wolf, P. G. (2012). Widespread triploidy in Western North American aspen (Populus tremuloides). *Plos One, 7*(10), e48406. doi: 10.1371/journal.pone.0048406

Mock, K. E., Rowe, C. A., Hooten, M. B., Dewoody, J., & Hipkins, V. D. (2008). Clonal dynamics in western North American aspen (Populus tremuloides). *Molecular Ecology, 17*(22), 4827-4844. doi: 10.1111/j.1365-294X.2008.03963.x

Mueggler, W. F. (1988). Aspen community types of the Intermountain Region. Gen. Tech. Rep. INT-250 (pp. 135 p.). Ogden, UT: U.S. Department of Agriculture, Forest Service, Intermountain Research Station.

Nicotra, A. B., & Davidson, A. (2010). Adaptive phenotypic plasticity and plant water use. *Functional Plant Biology, 37*(2), 117-127. doi: http://dx.doi.org/10.1071/FP09139

Nobel, P. S. (1999). *Physicochemical and environmental plant physiology*: Academic press.

Noss, R. F. (2001). Beyond Kyoto: Forest Management in a Time of Rapid Climate Change. *Conservation Biology, 15*(3), 578-590. doi: 10.1046/j.1523-1739.2001.015003578.x

Oren, R., Sperry, J. S., Katul, G. G., Pataki, D. E., Ewers, B. E., Phillips, N., & Schaefer, K. V. R. (1999). Survey and synthesis of intra- and interspecific variation in

stomatal sensitivity to vapour pressure defici. *Plant Cell and the Environment, 22*, 1515-1526.

Pärnik, T., Ivanova, H., Keerberg, O., Vardja, R., & Niinemets, Ü. (2014). Tree age-dependent changes in photosynthetic and respiratory CO2 exchange in leaves of micropropagated diploid, triploid and hybrid aspen. *Tree Physiol*, tpu043.

Peet, R. K. (1981). Forest vegetation of the Colorado front range. *Vegetatio, 45*(1), 3-75.

Pennington, R. E., Tischler, C. R., Johnson, H. B., & Polley, H. W. (1999). Genetic variation for carbon isotope composition in honey mesquite (Prosopis glandulosa). *Tree Physiol, 19*(9), 583-589.

Perala. (2004). Silvics of North America, Volume 2, hardwoods.pdf>.

R Core Team. (2014). R: A Language and Environment for Statistical Computing. Vienna, Austria: R Foundation for Statistical Computing. Retrieved from http://www.R-project.org/

Rehfeldt, G. E., Ferguson, D. E., & Crookston, N. L. (2009). Aspen, climate, and sudden decline in western USA. *Forest Ecology and Management, 258*(11), 2353-2364. doi: 10.1016/j.foreco.2009.06.005

Roden, J. S. (2003). Modeling the light interception and carbon gain of individual fluttering aspen (Populus tremuloides Michx) leaves. *Trees-Structure and Function, 17*(2), 117-126. doi: 10.1007/s00468-002-0213-3

Roden, J. S., & Pearcy, R. W. (1993a). The effect of flutter on the temperature of poplar leaves and its implications for carbon gain. *Plant Cell Environ, 16*(5), 571-577. doi: 10.1111/j.1365-3040.1993.tb00905.x

Roden, J. S., & Pearcy, R. W. (1993b). Effect of Leaf Flutter on the Light Environment of Poplars. *Oecologia, 93*(2), 201-207. doi: Doi 10.1007/Bf00317672

Roden, J. S., & Pearcy, R. W. (1993c). Photosynthetic Gas-Exchange Response of Poplars to Steady-State and Dynamic Light Environments. *Oecologia, 93*(2), 208-214. doi: Doi 10.1007/Bf00317673

Rogers, P. C., & Gale, J. A. (2017). Restoration of the iconic Pando aspen clone: emerging evidence of recovery. *Ecosphere, 8*(1), n/a-n/a. doi: 10.1002/ecs2.1661

Romme, W. H., Turner, M. G., Gardner, R. H., Hargrove, W. W., Tuskan, G. A., Despain, D. G., & Renkin, R. A. (1997). A rare episode of sexual reproduction in aspen (Populus tremuloides Michx.) following the 1988 Yellowstone fires. *Natural Areas Journal, 17*(1), 17.

Schneider, C. A., Rasband, W. S., & Eliceiri, K. W. (2012). NIH Image to ImageJ: 25 years of image analysis. *Nat Methods, 9*(7), 671-675.

Schoener, T. W. (1968). The Anolis Lizards of Bimini: Resource Partitioning in a Complex Fauna. *Ecology, 49*, 704-726.

Schreiber, S. G., Ding, C., Hamann, A., Hacke, U. G., Thomas, B. R., & Brouard, J. S. (2013). Frost hardiness vs. growth performance in trembling aspen: an experimental test of assisted migration. *Journal of Applied Ecology, 50*(4), 939-949. doi: 10.1111/1365-2664.12102

Segraves, K. A., & Anneberg, T. J. (2016). Species interactions and plant polyploidy. *Am J Bot, 103*(7), 1326-1335.

Seibt, U., Rajabi, A., Griffiths, H., & Berry, J. A. (2008). Carbon isotopes and water use efficiency: sense and sensitivity. *Oecologia, 155*(3), 441-454. doi: DOI 10.1007/s00442-007-0932-7

Sharkey, T. D. (1985). Photosynthesis in intact leaves of C3 plants: physics, physiology and rate limitations. *The Botanical Review, 51*(1), 53-105.

Shepperd, W., Binkley, D., & Bartos, D. (2000, 13–15 June 2000). Paper presented at the Sustaining Aspen in Western Landscapes: Symposium Proceedings, Fort Collins, CO.

Shepperd, W. D., Rogers, P. C., Burton, D., & Bartos, D. L. (2006). Ecology, Biodiversity, Management, and Restoration of Aspen in the Sierra Nevada. Gen. Tech. Rep. RMRS-GTR-178 (pp. 122 p.). Fort Collins, CO: U.S. Department of Agriculture, Forest Service, Rocky Mountain Research Station.

Shuttleworth, W. J. (1993). Evaporation. In D. R. Maidment (Ed.), *Handbook of Hydrology* (Vol. 4.1–4.53): McGraw-Hill.

Soltis, D. E., Segovia-Salcedo, M. C., Jordon-Thaden, I., Majure, L., Miles, N. M., Mavrodiev, E. V., Mei, W. B., Cortez, M. B., Soltis, P. S., & Gitzendanner, M. A. (2014). Are polyploids really evolutionary dead-ends (again)? A critical reappraisal of Mayrose et al. (2011). *New Phytologist, 202*(4), 1105-1117. doi: Doi 10.1111/Nph.12756

Sterck, L., Rombauts, S., Jansson, S., Sterky, F., Rouze, P., & Van de Peer, Y. (2005). EST data suggest that poplar is an ancient polyploid. *New Phytol, 167*(1), 165-170. doi: 10.1111/j.1469-8137.2005.01378.x

Thornley, J. H. (2002). Instantaneous canopy photosynthesis: analytical expressions for sun and shade leaves based on exponential light decay down the canopy and an acclimated non-rectangular hyperbola for leaf photosynthesis. *Ann Bot, 89*(4), 451-458.

Thuiller, W., Georges, D., & Engler, R. (2014). biomod2: Ensemble platform for species distribution modeling. Retrieved from http://CRAN.R-project.org/package=biomod2

Turner, M. G., Romme, W. H., & Tinker, D. B. (2003). Surprises and lessons from the 1988 Yellowstone fires. *Frontiers in Ecology and the Environment, 1*(7), 351-358.

Tyree, M. T., Patino, S., Bennink, J., & Alexander, J. (1995). Dynamic Measurements of Root Hydraulic Conductance Using a High-Pressure Flowmeter in the Laboratory and Field. *Journal of experimental botany, 46*(282), 83-94. doi: DOI 10.1093/jxb/46.1.83

Vitt, P., Havens, K., Kramer, A. T., Sollenberger, D., & Yates, E. (2010). Assisted migration of plants: changes in latitudes, changes in attitudes. *Biological Conservation, 143*(1), 18-27.

Von Caemmerer, S. v., & Farquhar, G. (1981). Some relationships between the biochemistry of photosynthesis and the gas exchange of leaves. *Planta, 153*(4), 376-387.

Wang, T., Hamann, A., Spittlehouse, D. L., & Murdock, T. Q. (2012). ClimateWNA-high-resolution spatial climate data for western North America. *Journal of Applied Meteorology and Climatology, 51*(1), 16-29.

Warren, D. L., Cardillo, M., Rosauer, D. F., & Bolnick, D. I. (2014). Mistaking geography for biology: inferring processes from species distributions. *Trends Ecol Evol, 29*(10), 572-580. doi: http://dx.doi.org/10.1016/j.tree.2014.08.003

Warren, D. L., Glor, R. E., & Turelli, M. (2008). Environmental Niche Equivalency versus Conservatism: Quantitative Approaches to Niche Evolution. *Evolution, 62*(11), 2868-2883. doi: 10.1111/j.1558-5646.2008.00482.x

White, J., & Vaughn, B. (2011). Stable Isotopic Composition of Atmospheric Carbon Dioxide (13C and 18O) from the NOAA ESRL Carbon Cycle Cooperative Global Air Sampling Network, 1990–2012, Version: 2013-04-05. University of Colorado, Institute of Arctic and Alpine Research (INSTAAR). *ftp. cmdl. noaa. gov/ccg/co2c13/flask/event/,(last access 21 September 2012)*.

Worrall, J. J., Egeland, L., Eager, T., Mask, R. A., Johnson, E. W., Kemp, P. A., & Shepperd, W. D. (2008). Rapid mortality of Populus tremuloides in southwestern Colorado, USA. *Forest Ecology and Management, 255*(3-4), 686-696. doi: DOI 10.1016/j.foreco.2007.09.071

Worrall, J. J., Marchetti, S. B., Egeland, L., Mask, R. A., Eager, T., & Howell, B. (2010). Effects and etiology of sudden aspen decline in southwestern Colorado, USA. *Forest Ecology and Management, 260*(5), 638-648. doi: DOI 10.1016/j.foreco.2010.05.020

Worrall, J. J., Rehfeldt, G. E., Hamann, A., Hogg, E. H., Marchetti, S. B., Michaelian, M., & Gray, L. K. (2013). Recent declines of Populus tremuloides in North America linked to climate. *Forest Ecology and Management, 299*, 35-51. doi: DOI 10.1016/j.foreco.2012.12.033

Zang, C., & Biondi, F. (2015). treeclim: an R package for the numerical calibration of proxy-climate relationships. *Ecography, 38*(4), 431-436 (V 431.437-413). doi: 10.1111/ecog.01335

APPENDICES

7. Appendices

Appendix S1: Data sources

The raw presence-absence data is the same dataset used by Worrall et al. (2013). Supplement 1 of Worrall et al. (2013) notes that the combined presence-absence dataset is obtained from inventory sample plots, ecology plots, and herbarium accessions. Of special note, there are some aspen locations whose presence may be confused with other species: for example, the Maritime Provinces of Canada do not distinguish between bigtooth aspen (*Populus grandidentata*) and trembling aspen.

Appendix S2: Methods for Climate Data Layer Creation

CLIMATE DATA

Climate layers (Table 4.2) were either used directly or calculated from datasets provided by WorldClim (Hijmans, et al., 2005). The spatial resolution for all data sources is thirty arc-seconds, or approximately 800 meters. This resolution, while coarser than the presence/absence data, is the finest scale of analysis for the models.

The specifics of the climate layers are as follows:

The Growing Degree Days metric represents the sum of monthly growing degree days (GDD) over 5°C for the year. GDD represents cumulative warmth for the year and is an index for the warmth of a site above a threshold degree of 5°C, which is used as a minimum threshold above which plants are most productive. This calculation is taken from Kira (1976), who originally referred to it as a ‘warmth index.'

Monthly GDD are created using the following scenarios using temperature maxima and minima adapted from Kira's warmth index (Kira, 1991):

a. When the minimum temperature of a month is above 5°C, all days in that month are assumed to be above temperature 5°C. Thus, GDD of the month is calculated as:

$$MonthGDD = (\frac{T\max + T\min}{2} - 5) * (days\_in\_month)$$

b. If the maximum temperature of a month is below 5°C, all days in that month are assumed to be below 5°C and the GDD of the month is 0:

$$MonthGDD = 0 * (days\_in\_month)$$

c. If the maximum and minimum temperatures span the 5°C threshold, then the number of days above 5°C was calculated using linear interpolation. When Tmax and Tmin are an equal magnitude from the 5°C threshold (e.g., 7.5°C and 2.5°C), this ratio would be 0.5; relative to 0.5, this ratio would increase (decrease) if Tmax (Tmin) were farther away from 5°C than Tmin (Tmax). So Month Growing Degrees would be ((Tmax + 5°C)/2 - 5°C).

$$MonthGDD = (\frac{T\max + 5}{2} - 5) * \frac{T\max - 5}{T\max - T\min} * (days\_in\_month)$$

Mean Annual Precipitation (MAP) represents the mean total yearly precipitation. Potential evapotranspiration represents the total PET in mm per year. The data source is WorldClim (Hijmans et al., 2005) where PET is calculated using the Hargreaves et al. (1985) model. Mean monthly temperature (Tmean), mean monthly temperature range (TD) and mean monthly extra-terrestrial radiation (RA, at top of atmosphere) were used to calculate mean PET for a raster of the world using this formula:

$$PET = 0.0023 * RA * (Tmean + 17.8) * TD^{0.5}$$

These data are summarized for the 1950 to 2000 period using available rasterized data available from WorldClim databases and extra-terrestrial radiation calculated where the solar constant, solar declination and the time of the year are used to determine RA (Allen et al., 1998). This RA value is dependent on latitude.

AET/MAP is actual evapotranspiration divided by MAP and is supplied by WorldClim.

PET/MAP is PET divided by MAP.

Precipitation seasonality represents the ratio of winter precipitation to summer precipitation. It is calculated using ArcGIS from monthly precipitation total summaries provided by WorldClim. Winter precipitation is represented by adding monthly precipitation totals for December, January, February and March. Summer precipitation is represented by adding monthly precipitation totals for June, July, August and September. The winter total is then divided by the summer total to produce Precip Seasonality.

Temperature Maximum and temperature minimum are the mean monthly maximum and minimum temperatures across the year.

TRNG represents the range of temperatures. It is calculated from the yearly average maximum (Tmax) and minimum (Tmin) data layers. It is also referred to as Trange_m14 in the MaxEnt outputs.

Appendix S3: Absence Data Boxplots

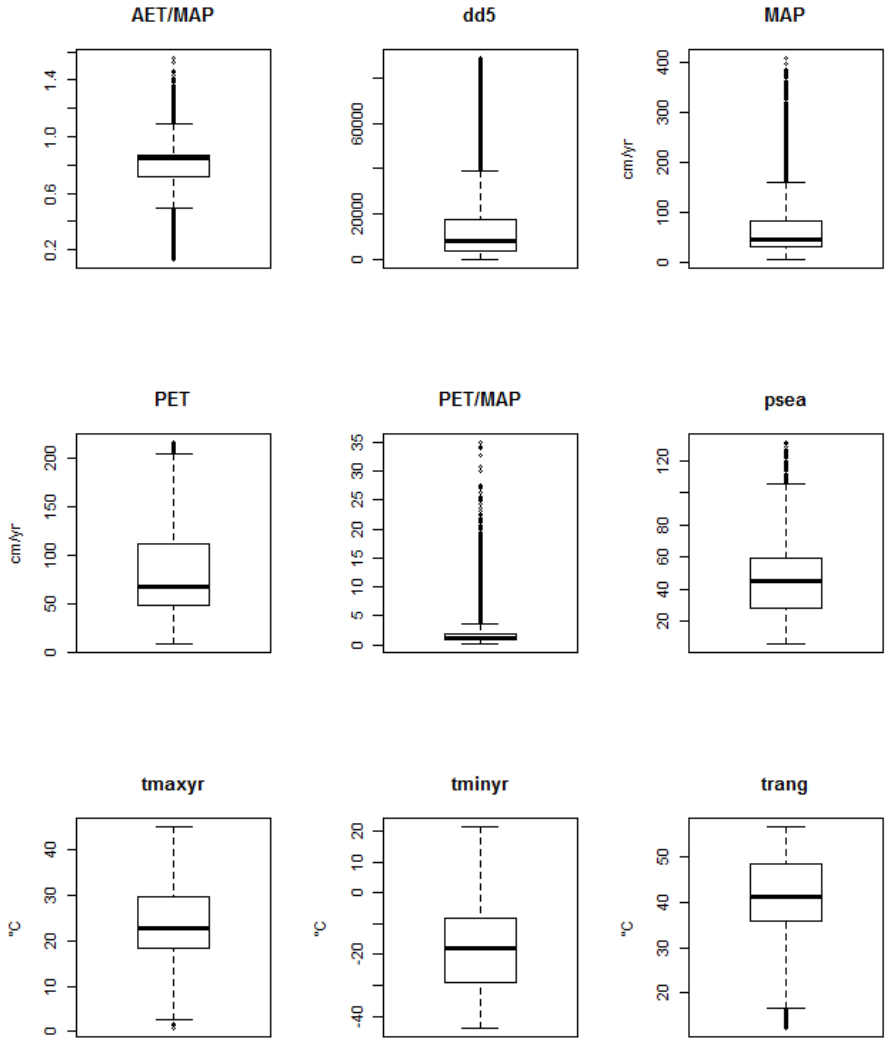

Figure 7.1 Boxplots of the absence data used in EP, NC and SC.

Appendix S4: Ensemble model methods

Table 7.1 Models included in ensemble (TSS>.6) listed by model type.

	EP	NC	SC
GBM	0	0	20
GLM	5	20	20
GAM	0	16	20
CTA	6	20	20
ANN	0	0	20
SRE	0	0	20
FDA	0	0	20
MARS	0	3	20
RF	20	20	20
MAXENT	12	20	20

Table 7.2 Average variable importance measured across all methods

	EP	NC	SC
AET/MAP	0.06	0.06	0.07
dd5	0.22	0.27	0.30
map	0.21	0.19	0.21
pet	0.25	0.44	0.83
PET/MAP	0.22	0.22	0.22
psea	0.04	0.03	0.07
tmaxyr	0.33	0.16	0.41
tminyr	0.29	0.24	0.20
trang	0.20	0.17	0.17

Table 7.3 Weighted average variable importance across all models

Weighted Variable Importance	EP	NC	SC
AET/MAP	0.05	0.03	0.07
dd5	0.18	0.26	0.30
map	0.14	0.08	0.21
pet	0.15	0.31	0.83
PET/MAP	0.15	0.17	0.22
psea	0.04	0.02	0.07
tmaxyr	0.21	0.13	0.41
tminyr	0.17	0.16	0.20
trang	0.12	0.14	0.17

Appendix S5: Photosynthetic meaurement methods supplemental, equations and calculations

A/C_i measurements:

C_i was calculated using the following equation from (Von Caemmerer & Farquhar):

$$C_i = \frac{(g_c - \frac{E}{2})c'_{an}) - A}{g_c + \frac{E}{2}}$$

where c'_{an} is the CO_2 flowing out of the chamber in μ mol mol^{-1}, E is the leaf transpiration rate (mol $m^2 s^{-1}$). g_c is defined as:

$$g_c = \frac{1}{1.6r_s + 1.37r_b}$$

where r_s is the stomatal resistance to water vapor and r_b is the boundary layer resistance to water vapor. r_s is defined as:

$$r_s = \frac{w_{leaf} - wm_{an}}{\frac{\Delta e u_s}{p}} - r_b$$

where w_{leaf} is the saturated water vapor concentration at leaf temperature, wm_{an} is the water vapor concentration out of the leaf chamber, Δe is the differential water vapor concentration (mbar, dilution corrected), u_s is the mass flow of air per m2 of leaf area (200 mol m^{-2} s^{-1}) and p is the atmospheric pressure (mBar). w_{leaf} is the saturated vapor pressure at the leaf surface (mBar) and is defined as:

$$w_{leaf} = \frac{e_s}{p}$$

where e_s is the saturated vapor pressure (mBar) at the leaf chamber temperature and p is the atmospheric pressure (mBar).

Leaf florescence

The theory behind fluorescence measurements is as follows (as described by Maxwell and Johnson (2000)): Chlorophyll absorbs light energy that is used to drive photosynthesis through photochemistry. If excess light energy is received by chlorophyll, it will be emitted as either heat energy, or as light; chlorophyll fluorescence is emitted light energy. The energy that is absorbed, emitted as heat, or emitted as light are in opposition and any increase in one results in a decrease in the others. Therefore, by measuring chlorophyll fluorescence, changes to either light absorption or heat dissipation can be extrapolated. A single measurement of fluorescence consists of multiple parts: first, a measurement of background fluorescence (F_0) is made, followed by a saturating pulse of light and a measurement of maximum fluorescence (F_m) and these data are recorded. Afterwards, an actinic light illuminates the sample and additional measurements at different intensities of light provide the background fluorescence (F_t) and maximum fluorescence (F'_m) under different light intensities.

Appendix S6: Hydraulic Conductance

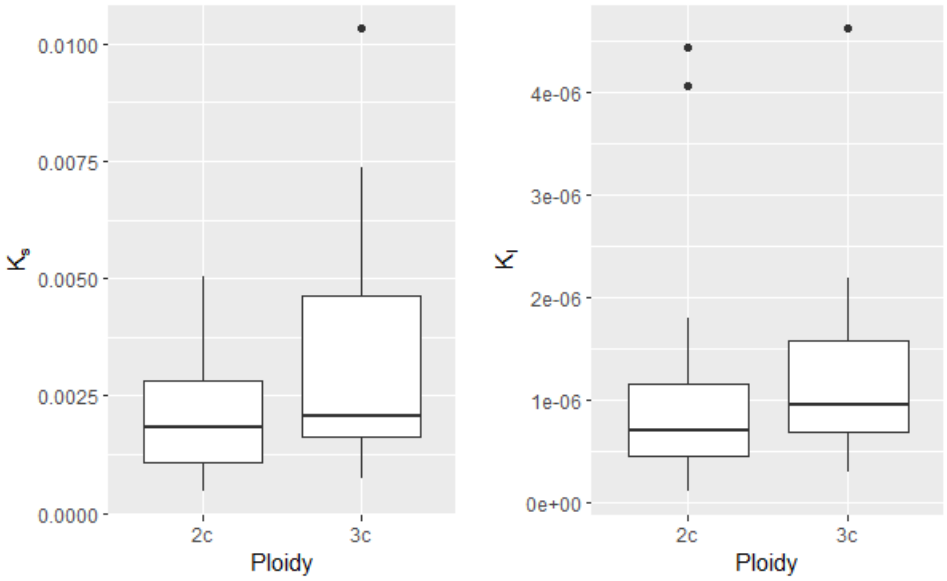

Figure 7.2 Measurements of Ks, and Kl were not statistically significantly different (likely due to small sample numbers, n = 40), but triploid aspen are consistently greater than diploids in each measurement.

Measurements of Ks, and Kl were not statistically significantly different (likely due to small sample numbers, n = 40), but triploid aspen are consistently greater than diploids in each measurement.

Appendix S7: Linear Mixed Model Methodology

Each of the linear mixed models followed one of the following model forms to address the question if the measurement differed between the ploidy types:

1) Fixed effect is ploidy and random effect clone. Measurement is the response variable and measured at ramet scale.

$$Y_{ijk} = \beta_0 + \beta_1 (I_p)_i + b_j + \varepsilon_{jk}$$

where:

Y_{ijk} is the measurement taken in the ith ploidy (diploid or triploid), in the jth clone, within the kth ramet,

β_0 is the mean of the measurement for diploids,

β_1 is the incremental effect to the measurement for triploids,

I_p is an indicator variable which is 1 if triploid and zero otherwise,

b_j is the random effect of the jth clone on the average of the measurement, $b_j \sim N(\sigma^2_b)$ and b_j and $b_{j'}$ are independent,

ε_{jk} is the random error term of the kth ramet of the jth clone, $\varepsilon_{jk} \sim N(0,\sigma^2)$ and ε_{jk} and $\varepsilon_{j'k'}$ are independent. In addition, it is assumed that ε_{jk} and b_j are independent.

2) Fixed effect is ploidy and random effect is ramet nested within clone. Measurement is the response variable and measured at the sub-ramet scale (for example, on a leaf).

$$Y_{ijkl} = \beta_0 + \beta_1(I_p)_i + b_j + \varepsilon_{jk} + \rho_{jkl}$$

where:

Y_{ijkl} is the measurement taken in the ith ploidy (diploid or triploid) in the jth clone, within the kth ramet, on the lth sub-ramet measurement

β_0 is the mean of the measurement for diploids

β_1 is the incremental effect to the measurement for triploids

I_p is an indicator variable which is 1 if triploid and zero otherwise

b_j is the random effect of the jth clone on the average of the measurement, b_j ~ N(σ^2_b) and b_j and $b_{j'}$ are independent.

ε_{jk} is the random effect of the jth clone and kth ramet on the average of the measurement. $\varepsilon_{jk} \sim N(0,\sigma^2)$ and ε_{jk} and $\varepsilon_{j'k'}$ are independent. In addition, it is assumed that ε_{ij} and b_j are independent.

ρ_{jkl} is the random error term of the jth clone in the kth ramet for the lth measurement, $\rho_{jkl} \sim N(0,\sigma^2)$ and ρ_{jkl} and $\rho_{j'k'l'}$ are independent. In addition, it is assumed that ρ_{jkl}, ε_{ijk} and b_j are independent.

3) Fixed effect is ploidy and a continuous variable with an interaction. The random effect is ramet nested within clone. The measurement is the response variable and measured at the sub-ramet scale (for example, on a leaf).

$$Y_{ijkl} = \beta_0 + \beta_1(I_p)_i + \beta_2 X_{ijkl} + \beta_3 X_{ijkl} + b_j + \varepsilon_{jk} + \rho_{jkl}$$

where:

Y_{ijkl} is the measurement taken in the ith ploidy (diploid or triploid) in the jth clone, within the kth ramet, on the lth sub-ramet measurement

β_0 is the mean of the measurement for diploids

β_1 is the incremental effect to the measurement for triploids

β_2 is the slope of the measurement for diploids

β_3 is the incremental change in slope of the measurement for triploids

X_{ijkl} is the value of the continuous variable in the fixed effects (not ploidy)

I_p is an indicator variable which is 1 if triploid and zero otherwise

b_j is the random effect of the jth clone on the average of the measurement, b_j ~ $N(\sigma^2_b)$

and b_j and $b_{j'}$ are independent.

ε_{jk} is the random effect of the jth clone and kth ramet on the average of the measurement. $\varepsilon_{jk} \sim N(0,\sigma^2)$ and ε_{jk} and $\varepsilon_{j'k'}$ are independent. In addition, it is assumed that ε_{ij} and b_j are independent.

ρ_{jkl} is the random error term of the jth clone in the kth ramet for the lth measurement, $\rho_{jkl} \sim N(0,\sigma^2)$ and ρ_{jkl} and $\rho_{j'k'l'}$ are independent. In addition, it is assumed that ρ_{jkl}, ε_{ijk} and b_j are independent.

4) Fixed effect is ploidy and random effect is curve ID. Measurement is the response variable and measured as PAR is increased.

$$Y_{ijkl} = \beta_0 + \beta_1(I_p)_i + b_j + \rho_{jkl}$$

where:

Y_{ijkl} is the measurement taken in the ith ploidy (diploid or triploid) in the jth clone, within the kth ramet, on the lth sub-ramet measurement

β_0 is the mean of the measurement for diploids

β_1 is the incremental effect to the measurement for triploids

I_p is an indicator variable which is 1 if triploid and zero otherwise

b_j is the random effect of the lth curve on the average of the measurement, b_j ~ $N(\sigma^2_b)$ and b_j and $b_{j'}$ are independent.

ρ_{jkl} is the random error term of the jth curve in the kth ramet in a clone for the lth measurement, $\rho_{jkl} \sim N(0,\sigma^2)$ and ρ_{jkl} and $\rho_{j'k'l'}$ are independent. In addition, it is assumed that ρ_{jkl}, ε_{ijk} and b_j are independent.

(continued)

Table 7.4 Models used for our mixed effect models

Measurement	Model Form	Model Adjustments
Basal Area per ground area (m^2/ha)	1	
Canopy Coverage (% open canopy)	1	
DBH (cm)	1	
Tree Height (meters)	1	
Leaf Area Index (LAI, leaf area per unit ground)	1	
Leaf Area Distal to Branch Segment (m2)	1	
Hydraulic Conductivity, Kh (kg m^2 s^{-1} MPa^{-1})	1	
Specific Conductivity , Ks (kg m^{-1} s^{-1} MPa^{-1})	1	
Hydraulic Conductivity normalized by leaf area, KL (kg m^{-1} s^{-1} MPa^{-1})	1	
Leaf Area (cm^2)	1	residuals calculated separately by ploidy type
Leaf Dry Mass (grams)	1	

(continued)

Leaf Mass per Area (LMA, grams/cm^2)	1	
Leaf Chlorophyll content (SPAD, a unitless index)	1	
Leaf Stomatal length (μm)	2	
Leaf Stomatal density (count per mm^2)	2	
Leaf Stomatal conductance, g_s, (mmol m^{-2} sec^{-1})	3	
Stomatal conductance, g_s, (mmol m^{-2} sec^{-1}) with log(D) as fixed effect	3	
V_{cmax}	1	
J_{max}	1	
R_d	1	
Γ*	1	
K_m	1	
Φ_{PSII} (Dark adapted)	4	
Φ_{PSII} (Light adapted)	4	compound correlation structure
J (light adapted)	4	
July 2015 α (from curves fit individually)	1	
July 2015 ETR_{max} (from curves fit individually)	1	
June 2016, α (from curves fit individually)	1	
June 2016, ETR_{max} (from curves fit individually)	1	
$\delta^{13}C$	2	

(continued)

C_i	2	
C_i/C_a	2	
iWUE	2	
Leaf N % mass	2	
Leaf C% mass	2	
C:N	2	

Appendix S8: Variance Components

Using methods described in Edwards et al. (2008) we calculated the variance components for ploidy, clone, ramet and leaf trait measurements.

Table 7.5 Summary of variance component contributions

% Fixed Effect (Ploidy) Variance	% Clone Variance	% Ramet Variance	% Leaf Variance
13.7	29.7	51.3	26.4

Table 7.6 Individual variance component contributions

Measurement	n	% Fixed Effect (Ploidy) Variance	% Clone Variance	% Ramet Variance	% Leaf Variance
Basal Area per ground area (m^2/ha)	52	9.5	90.5		
Canopy Coverage (% open canopy)	52	0.0	100.0		
DBH (cm)	51	0.0	0.0	100.0	
Tree Height (meters)	51	2.1	1.4	96.5	
Leaf Area Index (LAI, leaf area per unit ground)	42	6.0	42.4	51.6	
Leaf Area Distal to Branch Segment (cm^2)	40	1.5	12.6	85.9	
Hydraulic Conductivity, Kh (kg m^2 s^{-1} MPa^{-1})	40	5.4	12.6	82.0	

Specific Conductivity , Ks (kg m^{-1} s^{-1} MPa^{-1})	40	8.0	43.6	48.4	
Hydraulic Conductivity normalized by leaf area, Kl (kg m^{-1} s^{-1} MPa^{-1})	40	0.7	16.5	82.7	
Area per leaf (cm^2)	52	32.2	57.4	10.5	
Dry Mass per leaf (grams)	52	39.2	52.9	7.8	
Leaf Mass per Area (LMA, grams/cm^2)	52	24.4	46.8	28.8	
Chlorophyll content (SPAD, a unitless index)	51	27.9	54.1	17.9	
Stomatal length (μm)	52	26.6	31.3	6.6	35.4
Stomatal density (count per mm^2)	52	1.8	28.7	11.5	58.0
Stomatal conductance, g_s, (mmol m^{-2} sec^{-1})	261	3.0	5.1	9.1	82.7
Stomatal conductance, g_s, (mmol m^{-2} sec^{-1}) with log(D) as fixed effect	261	27.4	3.8	6.8	62.0
V_{cmax}	22	0.2	12.8	87.0	
J_{max}	22	17.0	41.2	41.7	
R_d	22	2.2	0.0	97.8	

Γ*	22	15.0	53.2	31.9	
K_m	22	15.3	51.1	33.6	
Φ_{PSII} (Dark adapted)	1142	0.6	22.5	77.0	
Φ_{PSII} (Light adapted)	1017	43.6	5.7	50.7	
J (light adapted)	1017	17.8	0.0	82.2	
July 2015 α (from curves fit individually)	110	2.4	45.1	52.5	
July 2015 ETR_{max} (from curves fit individually)	110	3.6	22.7	73.7	
June 2016, α (from curves fit individually)	18	32.3	32.0	35.7	
June 2016, ETR_{max} (from curves fit individually)	18	6.6	0.0	93.4	
$\delta^{13}C$	63	23.0	32.3	40.7	4.0
C_i	63	23.0	32.3	40.7	4.0
C_i/C_a	63	23.0	32.3	40.7	4.0
iWUE	63	23.0	32.3	40.7	4.0
Leaf N % mass	63	10.9	17.7	58.5	12.9
Leaf C% mass	63	2.2	0.0	84.1	13.7
C:N	63	16.2	37.9	36.0	10.0